


Adult alcohol drinking and emotional tone are mediated by neutral sphingomyelinase during development in males

Liubov S. Kalinichenko¹, Christiane Mühle¹, Tianye Jia ^{2,3}, Felix Anderheiden¹, Maria Datz¹, Anna-Lisa Eberle¹, Volker Eulenburg⁴, Jonas Granzow¹, Martin Hofer¹, Julia Hohenschild¹, Sabine E. Huber¹, Stefanie Kämpf¹, Georgios Kogias¹, Laura Lacatusu¹, Charlotte Lugmair¹, Stephen Mbu Taku¹, Doris Meixner¹, Nina-Kristin Sembritzki¹, Marc Praetner^{1,5}, Cosima Rhein^{1,6}, Christina Sauer¹, Jessica Scholz¹, Franziska Ulrich¹, Florian Valenta¹, Esther Weigand¹, Markus Werner¹, Nicole Tay², Conor J. Mc Veigh⁷, Jana Haase⁷, An-Li Wang⁸, Laila Abdel-Hafiz⁸, Joseph P. Huston⁸, Irena Smaga⁹, Malgorzata Frankowska⁹, Malgorzata Filip⁹, Anbarasu Lourdasamy¹⁰, Philipp Kirchner¹¹, Arif B. Ekici¹¹, Lena M. Marx¹, Neeraja Puliparambil Suresh¹, Renato Frischknecht¹², Anna Fejtova¹, Essa M. Saied^{13,14}, Christoph Arenz¹³, Aline Bozec^{15,16}, Isabel Wank¹⁷, Silke Kreitz¹⁷, Andreas Hess¹⁷, Tobias Bäuerle¹⁸, Maria Dolores Ledesma¹⁹, Daniel N. Mitroi¹⁹, André M. Miranda^{20,21}, Tiago Gil Oliveira^{20,21}, Bernd Lenz^{1,22}, Gunter Schumann^{2,3,23,†}, Johannes Kornhuber^{1,†}, Christian P. Müller ^{1,24,†,*}

¹Department of Psychiatry and Psychotherapy, University Clinic, Friedrich-Alexander-University of Erlangen-Nürnberg, Schwabachanlage 6, Erlangen 91054, Germany,

²The Centre for Population Neuroscience and Stratified Medicine (PONS), ISTBI, Fudan University, Shanghai 200433, China,

³PONS Centre and SGDP Centre, Institute of Psychiatry, Psychology and Neuroscience, King's College London, London SE5 8AB, UK,

⁴Department for Anesthesiology and Intensive Care, Faculty of Medicine, University of Leipzig, Leipzig 04103, Germany,

⁵Biomedical Center, Institute of Cardiovascular Physiology and Pathophysiology, Faculty of Medicine, Ludwig-Maximilians-Universität München, Munich 82152, Germany,

⁶Department of Psychosomatic Medicine and Psychotherapy, Friedrich-Alexander-University of Erlangen-Nürnberg, Erlangen 91054, Germany,

⁷School of Biomolecular and Biomedical Science, UCD Conway Institute, University College Dublin, Dublin 4, Ireland,

⁸Center for Behavioral Neuroscience, Institute of Experimental Psychology, University of Düsseldorf, Düsseldorf 40225, Germany,

⁹Department of Drug Addiction Pharmacology, Maj Institute of Pharmacology, Polish Academy of Sciences, Smetna 12, Kraków 31-343, Poland,

¹⁰Division of Child Health, Obstetrics and Gynaecology, School of Medicine, University of Nottingham, Nottingham NG7 2UH, UK,

¹¹Institute of Human Genetics, Friedrich Alexander University of Erlangen-Nuremberg (FAU), Erlangen 91054, Germany,

¹²Department of Biology, Animal Physiology, Friedrich-Alexander-University of Erlangen-Nürnberg, Erlangen 91058, Germany,

¹³Institute for Chemistry, Humboldt University, Berlin 12489, Germany,

¹⁴Chemistry Department, Faculty of Science, Suez Canal University, Ismailia 41522, Egypt,

¹⁵Department of Internal Medicine 3—Rheumatology and Immunology, Friedrich-Alexander-University of Erlangen-Nürnberg, Erlangen 91054, Germany,

¹⁶Deutsches Zentrum für Immuntherapie (DZI), Erlangen 91054, Germany,

¹⁷Department of Experimental and Clinical Pharmacology and Toxicology, Emil Fischer Center, Friedrich-Alexander-University of Erlangen-Nuremberg (FAU), Erlangen, Germany,

¹⁸Preclinical Imaging Platform Erlangen, Institute of Radiology, University Hospital Erlangen, Erlangen 91054, Germany,

¹⁹Centro Biología Molecular Severo Ochoa (CSIC-UAM), Madrid 28040, Spain,

²⁰School of Medicine, Life and Health Sciences Research Institute (ICVS), University of Minho, Campus Gualtar, Braga 4710-057, Portugal,

²¹ICVS/3B's—PT Government Associate Laboratory, Braga/Guimarães 4710-057, Portugal,

²²Department of Addictive Behavior and Addiction Medicine, Central Institute of Mental Health (CIMH), Medical Faculty Mannheim, Heidelberg University, J5, Mannheim 68159, Germany,

²³Department of Psychiatry and Psychotherapie, CCM, PONS Centre, Charite Mental Health, Charite Universitaetsmedizin Berlin, Berlin 10117, Germany,

²⁴Centre for Drug Research, Universiti Sains Malaysia, 11800 Minden, Penang, Malaysia

*Corresponding author: Department of Psychiatry and Psychotherapy, University Clinic, Friedrich-Alexander University Erlangen-Nürnberg, Schwabachanlage 6, Erlangen 91054, Germany. Email: Christian.Mueller@uk-erlangen.de

†These authors contributed equally to this study.

Abstract

Alcohol use, abuse, and addiction, and resulting health hazards are highly sex-dependent with unknown mechanisms. Previously, strong links between the *SMPD3* gene and its coded protein neutral sphingomyelinase 2 (NSM) and alcohol abuse, emotional behavior, and bone defects were discovered and multiple mechanisms were identified for females. Here we report strong sex-dimorphisms for central, but not for peripheral mechanisms of NSM action in mouse models. Reduced NSM activity resulted in enhanced alcohol consumption in males, but delayed conditioned rewarding effects. It enhanced the acute dopamine response to alcohol, but decreased monoaminergic systems adaptations to chronic alcohol. Reduced NSM activity increased depression- and anxiety-like behavior, but was not involved in alcohol use for the self-management of the emotional state. Constitutively reduced NSM activity impaired structural development in the brain and enhanced lipidomic sensitivity to chronic alcohol. While the central effects were mostly

opposite to NSM function in females, similar roles in bone-mediated osteocalcin release and its effects on alcohol drinking and emotional behavior were observed. These findings support the view that the NSM and multiple downstream mechanism may be a source of the sex-differences in alcohol use and emotional behavior.

Key words: neutral sphingomyelinase; osteocalcin; depression; alcohol; anxiety.

Introduction

Alcohol abuse is a wide spread phenomenon that may result in addiction, a psychiatric disorder with still poor pharmacotreatment options (GBD 2018). In regular non-addicted consumers, alcohol is not predominantly used for its euphoric effects, but rather instrumentalized to achieve behavioral goals that would not be achievable or require a higher work load without the drug (Müller and Schumann 2011a, 2011b; Müller 2020). However, these goals significantly change in addicts (Müller et al. 2021). One of the most frequently reported instrumentalization goals is the management of an aversive affective state, which includes spontaneous or induced depression and anxiety (Müller et al. 2021). A mechanistic base for alcohol consumption to self-manage a genetically induced depression is the re-establishment of sphingolipid and monoamine homeostasis in the brain (Müller et al. 2017; Müller and Kornhuber 2017).

Alcohol use, abuse, addiction, and resulting health hazards are highly sex-dependent (GBD 2018). Males use and abuse alcohol for other reasons and subserved by distinct neurobiological mechanisms than females (Carroll and Lynch 2016; Sanchis-Segura and Becker 2016). Also instrumentalization goals appear to be sex-dependent (Hilderbrand and Lasek 2018; Turner et al. 2018; Müller et al. 2021). A lack of sex-specific understanding of alcohol neuropsychopharmacology may be one reason that has hampered the development of a personalized treatment of alcohol addiction.

Sphingolipids are among the most abundant lipids of the brain (Holthuis et al. 2001), where they critically shape appearance and dynamics of neuronal membranes. They form highly dynamic ceramide-enriched lipid platforms, which accommodate functional neurotransmitter receptors at the neuronal synapse and determine their function (Kornhuber et al. 2014; Schneider et al. 2017). Brain ceramides exert a crucial role on emotional behavior (Gulbins et al. 2013, 2018; Zoicas, Huber, et al. 2020) and learning and memory (Huston et al. 2016; Kalinichenko et al. 2021). A disruption of the brain sphingolipid rheostat may also give rise to psychiatric disorders such as depression (Gulbins et al. 2013, 2018) or alcohol addiction (Müller et al. 2017). Sphingomyelinases catalyze the turnover of highly abundant sphingomyelins to ceramides. Acid- (ASM), basic-, and neutral sphingomyelinase (NSM) have been distinguished, related to their optimal pH-value (Hannun and Obeid 2008). We have previously reported an association of NSM-2 coding gene SMPD3 haplotypes with alcohol use, depression and bone defects in a cohort of 456,693 male and female human individuals. A functional analysis showed multiple syndrome interactions

in females. However, sphingolipid systems in the brain show a strong sex-dimorphism (Gulbins et al. 2013; Zoicas, Schumacher, et al. 2020), which may be also responsible for the gender bias in alcohol addiction and depression. Here we describe a distinct role of NSM-2 in male alcohol use and in emotional behavior, which is together with its downstream neurochemical, lipidomic, and anatomical mechanisms largely different from females.

Materials and methods

Ethics statement

The experiments on rodents were carried out in accordance to the European Communities Council Directive (86/609/EEC) and National Institutes of Health guidelines for the humane treatment of animals and approved by the German Animal Protection Law Authorities (LANUV), Regierung von Düsseldorf and Regierung von Unterfranken.

Animals

Male transgenic mice with a heterozygous knock out of NSM activity (fro, fragilis ossium) and male wild type (WT) mice from the same litter, or male C57Bl6 mice, all aged 8–15 weeks, were used in the experiments (Aubin et al. 2005; Kalinichenko et al. 2021). Due to bone disorders developing in homozygous knock out mice (Aubin et al. 2005), they were not used in the study. The mice were kept under a normal light–dark cycle (2–5 per cage or single housed when required by the experiment; light off 07:00 pm–07:00 am). All animals had free access to food and water.

Alcohol-related behavior in mice

Alcohol drinking

Alcohol drinking pattern was tested in naïve male fro and WT mice (fro: $n=17$; WT: $n=20$) using a 2-bottle free-choice drinking paradigm. Mice were single housed and each cage was equipped with 2 bottles constantly available, one of which contained tap water and the other bottle contained alcohol in various concentrations. After an acclimatization period of 2 weeks to establish a water drinking baseline, animals received alcohol at increasing concentrations of 2, 4, 8, 12, and 16 vol. % for 4 days each. Bottles were changed and weighed daily. The consumed amount of alcohol and water relative to body weight and the preference vs. water were measured (Easton, Lucchesi, Lourdasamy, et al. 2013; Zheng et al. 2016; Müller et al. 2017).

Alcohol drinking behavior—pharmacology

To check the effects of an acute pharmacological inhibition of NSM on the emotional state of animals,

naïve male C57Bl6 mice ($n = 8/\text{group}$) were continuously administered with the selective NSM inhibitor GW4869 (Sigma) via Alzet osmotic mini pumps (model 1004; 28-day delivery; DURECT Corporation). Mini pumps were filled with a solution of GW4869 in 2.5% DMSO and implanted into the lower back of animals under isoflurane anesthesia (Isoflurane; Baxter, Germany; 5% induction, 2% maintenance). Mini pumps delivered the substance in the dose of 2 mg/kg/day. Control animals were implanted with vehicle-containing pumps. After the implantation, the animals were single housed with 2 water bottles and left for recovery. After 2 weeks, the animals were exposed to alcohol on the model of 2-bottle free-choice paradigm as mentioned above. The concentration of alcohol gradually increased from 2 to 16% every 2 days. Then, a concentration of 16% was kept for 5 days. The consumed amount of alcohol relative to body weight and the preference vs. water were measured during the whole experiment (Müller et al. 2017; Kalinichenko et al. 2021).

Conditioned place preference—alcohol

The establishment of conditioned place preference (CPP) for alcohol was tested in treatment naïve male fro and WT mice (fro: $n = 10$; WT: $n = 9$). The 2 TSE Place Preference test boxes (TSE Systems) with 3 compartments were composed of nontransparent polyvinyl chloride with standard inside dimensions (40 × 15 cm). The floor of the left chamber was covered with a smooth black rubber mat and the floor of the right chamber was covered with a patterned black rubber mat, whereas the center chamber was not covered and colored white. The system automatically recorded the number of entries, the time spent in the compartment and the distance moved in each compartment for each trial using high-resolution infrared sensors. An unbiased design was used in which half of the mice were conditioned to their preferred compartment, and half to their nonpreferred compartment. Animals were injected with either saline or alcohol (2 g/kg, 10 mL/kg, i.p.) immediately before each trial, and placed into the CPP boxes for conditioning/pseudoconditioning trials (Easton, Lucchesi, Mizuno, et al. 2013; Kalinichenko et al. 2021).

The CPP experiment involved 4 phases: a habituation trial (1 session), a preconditioning testing (baseline, Bl), conditioning trials (14 sessions), and preference tests (3 sessions, T1–T3). Habituation: The habituation session was intended to acclimatize the mice to the test procedure and apparatus prior to commencing the experiment. Mice were injected with saline and placed in the center compartment with free access to all three compartments for 20 min. Baseline test: The pretest was designed to establish a baseline level of preference for each individual. Mice were conditioned to either their preferred or nonpreferred compartment using a counterbalanced experimental design. Mice were injected with saline and placed in the center compartment with free

access to all three compartments for 20 min. *Conditioning trials:* Conditioning trials were performed in pairs; odd numbered pairings were conditioned with alcohol (2 mg/kg, i.p.) and even numbered pairings were conditioned with saline, balanced across groups. All animals received seven pairings with saline and 7 pairings with alcohol. Mice were injected with either saline or alcohol and introduced into 1 of the 2 conditioning compartments, with restricted access, for 5 min. *Preference tests:* Preference tests were systematically performed after 1 (T1), 3 (T2), and 7 (T3) conditioning/pseudoconditioning trials to monitor the time course of CPP establishment. Before each test, mice were injected with saline and placed in the center compartment with free access to all three compartments for 20 min. The time spent in the conditioning/pseudoconditioning compartment, the entries into these compartments, and conditioned locomotor activity were measured to estimate mechanisms driving a potential CPP (Easton, Lucchesi, Lourdasamy, et al. 2013; Kalinichenko et al. 2021).

In order to test the NSM effect on the expression of an alcohol-CPP, we measured the effects of an acute pharmacological inhibition of NSM activity on this parameter. For this purpose, naïve male C57Bl6 mice ($n = 9\text{--}10/\text{group}$) were conditioned for an alcohol CPP as described above, but with only 4 conditioning and four pseudoconditioning trials. Before the single test trial, they were treated with 2 selective NSM inhibitors, ES048 (400 ng/kg) and GW4869 (2 mg/kg, Sigma) (Kalinichenko et al. 2021), or vehicle and CPP was measured as described above.

Conditioned place preference—food

The establishment of CPP for food was tested in treatment naïve male fro and WT mice as described above (fro: $n = 10$; WT: $n = 9$). In order to familiarize animals with the new food, animals received a small amount of the conditioning food (~5 g/cage) in their home cage for 60 min 3 and 4 days before the conditioning procedure started. During the 20 min conditioning trials, ~1 g of a specific fat-carbohydrate mixture (FMD) [35:65 sunflower oil/maltodextrin; 24.3 kJ/g (5.8 kcal/g)] (Hess et al. 2019), was placed in a small petri dish in the middle of the conditioning compartment. During pseudoconditioning trials, the petri dish was left empty. The amount of food consumed during the condition trials was measured manually. The time spent in the conditioning/pseudoconditioning compartment, the entries into these compartments, and conditioned locomotor activity were recorded to estimate mechanisms driving a potential CPP (Easton, Lucchesi, Mizuno, et al. 2013; Hess et al. 2019).

In-vivo microdialysis

The experiment was performed on naïve male fro and WT mice (fro: $n = 6$; WT: $n = 9$). For cannula implantation, the mice were deeply anesthetized with isoflurane (4–5% for initiation and 2–3% for maintenance, O₂ at

2 L/min) and 1% lidocaine, 0.1 mL, (s.c.) for local anesthesia. Two guide cannulas (Microbiotech/se AB) were aimed at the dorsal hippocampus (DH; A: -2.1 ; L: ± 1.2 ; V: -1.1) and the nucleus accumbens (Nac; A: $+1.2$; L: ± 1.6 ; V: -4.3 ; angle $\pm 10^\circ$ from midline) using coordinates relative to bregma (Franklin and Paxinos 1997). The cannulas were fixed using two anchor screws (stainless steel, $d = 1.4$ mm) and dental cement. After the surgery 0.01 mL Rimadyl (5 mg/kg Carprofen) per 10 g body weight was given s.c. for analgesia; and 0.1 mL physiological saline was injected to restore fluid balance. Animals were kept warm during and after the surgery, afterwards returned to their home cages and monitored daily. The animals were given at least 5 days between the surgery and dialysis and were handled daily for 5 min/animal (Mielenz et al. 2018; Kalinichenko et al. 2019).

On the day of the experiment, microdialysis probes with membrane length of 1 mm were inserted into the guide cannula under a short (1–2 min) isoflurane narcosis (O_2 at 2 l/min, Isoflurane at 3–5%). After probe insertion, each animal was placed into a Plexiglas chamber ($21 \times 21 \times 30$ cm) with water ad libitum and room temperature 19–22 °C. The probes were connected to a microinfusion pump (CMA 400, Carnegie) and were perfused with artificial cerebrospinal fluid (Carl Roth GmbH) at room temperature and the flow rate of 1.5 μ L/min. The perfusion was allowed to stabilize for 2 h until a stable baseline was achieved. Then, samples were collected every 20 min into vials with 2.73 μ L of antioxidant (0.1 M perchloric acid) and 500 pg dihydroxybenzylamine as internal standard (Sigma/Carl Roth GmbH). First three samples were used to measure baseline quantities of the neurotransmitters dopamine (DA), serotonin (5-HT) and norepinephrine (NE) (Amato et al. 2020). After 1 h, an alcohol stimulus was applied (2 g/kg, i.p., $v_{inj} = 10$ mL/kg) and further six samples were collected. Once the microdialysis experiment was completed, the animal was sacrificed by cervical dislocation. The brain was isolated, and the localization of the probes was verified. Only samples from the animals with probes placed within the DH and Nac were considered for further analysis.

All samples were analyzed using HPLC with electrochemical detection to measure DA, 5-HT and NE levels. The column was an ET 125/2, Nucleosil 120-5, C-18 reversed phase column (Macherey & Nagel). The mobile phase consisted of 75 mM NaH_2PO_4 , 4 mM KCl, 20 μ M EDTA, 1.5 mM sodium dodecylsulfate, 100 μ L/l diethylamine, 12% alcohol, and 12% acetonitrile adjusted to pH 6.0 using phosphoric acid (Carl Roth GmbH). The electrochemical detector (Intro) was set at 500 mV vs. an ISAAC reference electrode (Antec) at 30 °C. This setup allows simultaneous measurement of DA, 5-HT, and NE (Amato et al. 2020; Kalinichenko et al. 2021).

Monoamine receptor expression

Alcohol or water drinking was established in naïve male fro and WT mice using a 2-bottle free-choice drinking paradigm as described above (fro: $n = 6/6$; WT: $n = 6/4$).

After 12 days drinking of 16 vol.% alcohol, animals were sacrificed and the ventral striatum (vStr) was isolated and immediately frozen on dry ice. The samples were stored at -80 °C until further analysis. RNA isolation from the samples was performed using the RNeasy Mini Kit (Qiagen) according to manufacturers' instructions. cDNA was generated from 1 μ g RNA using the SuperScript VILO cDNA Synthesis Kit (ThermoFisher) according to manufacturers' instructions. Quantitative real-time PCR was performed using a LightCycler 480 real-time PCR system (Roche, Germany). In detail, qPCR reactions contained 5 μ L TaqMan FastStart Advanced Master Mix (ThermoFisher), 0.5 μ L of FAM/VIC 20 \times , 2 μ L RNA-free water, and 2.5 μ L diluted cDNA (corresponding to 12.5 ng RNA) in a total volume of 10 μ L. Temperature profile used was: 35 cycles of amplification (95 °C for 30 s, 95 °C for 15 s, 60 °C for 60 s) followed by 40 °C for 10 s and by melting curve analysis. After run, PCR product specificity was assessed by the inspection of single peak melting curves, and threshold cycles (Ct) were determined with the second derivative maximum method using the LightCycler 480 software (release 1.5.0). The following TaqMan's were used for the reaction: SERT, Assay ID Mm00439391_m1; 5-HT1a: Assay ID Mm00434106_s1; 5-HT2a: Assay ID Mm00555764_m1; 5-HT2c: Assay ID Mm00434127_m1; 5-HT3a: Assay ID Mm00442874_m1; DAT, Assay ID Mm00438388_m1; D1: Assay ID Mm02620146_s1; D2: Assay ID Mm00438545_m1 (ThermoFisher) (Kalinichenko et al. 2021).

Serotonin uptake in synaptosomes

Crude synaptosomes (P2 membrane fractions) were prepared as described previously (Brown et al. 2018). Briefly, brains from male mice were rapidly removed and dissected. Individual brain regions, i.e. ventral hippocampus (VH) and DH and vStr were homogenized in ice-cold homogenization buffer (0.32 M sucrose, 5 mM Tris pH 7.4, and 1 mM EDTA buffer) using a Dounce homogenizer with a loose-fitted pestle. Homogenates were transferred to centrifuge tubes and large cell debris were removed by centrifugation at 1,300g for 5 min at 4 °C. Supernatants were transferred to new tubes and centrifuged at 17,000g at 4 °C for 10 min. The resulting P2 pellet was washed once in homogenization buffer and centrifuged as before, aliquots for protein assay (BCA) were collected. The remaining crude synaptosomes were resuspended in ice-cold transport buffer (TB, 10 mM HEPES, 150 mM NaCl, 2 mM KCl, 1 mM $CaCl_2$, 1 mM $MgCl_2$, 10 mM glucose) and diluted. Aliquots of synaptosomes (25–50 μ g/well) were preincubated at 37 °C in 200 μ L TB transport buffer containing 100 mU/mL bacterial sphingomyelinase (BSM) in 24-well plates for 60 min. [3H]-5-HT (PerkinElmer) was then added to each well to give a final concentration of 20 nM. The incubation was terminated after 10 min by addition of ice-cold transport buffer containing 1 μ M escitalopram and filtration onto a Microbeta 1450 Filtermat A using an Inotech Harvester. Filters were rapidly washed three times with transport

buffer and dried overnight. Dried filters were immersed in scintillation fluid and counted by scintillation spectrometry using a Wallac Microbeta counter. Counts for 5-HT transporter (SERT) specific [^3H]-5-HT uptake were determined by subtracting counts from parallel assays in the presence of 1 μM escitalopram (Kalinichenko et al. 2021).

Emotional behavior—naïve fro

Naïve male mice (fro: $n=8$ vehicle treated/11 corticosterone treated; WT: $n=11$ vehicle treated/11 corticosterone treated) were tested using a battery of behavioral tests in the following order: open field (OF), light-dark box, elevated plus maze, novelty suppressed feeding (NSF), forced swim, and sucrose preference tests (SPT). In order to test NSM effects in stressed animals, part of the animals were treated with corticosterone (0.25 mg/mL) in drinking water 7 days before and during testing (control: only drinking water; Gulbins et al. 2013). All tests were performed on separate days between 09:00 and 16:00 h. Mice were tested in a pseudorandom order and were moved to the behavioral suite adjacent to the housing room at least 1 h before testing. Each test apparatus was cleaned with 70% ethanol between subjects to avoid any olfactory cues influencing behaviors. Mice were returned to their home cages at the end of each test and allowed to recover for at least 2 days before further testing. Behaviors for all tests were recorded for subsequent scoring (Müller et al. 2017; Kalinichenko et al. 2021).

Open Field: Each mouse was placed in a square white acrylic arena (50 \times 50 cm), facing an outer wall, for 20 min and allowed to freely explore the arena. White light of 100 lx was evenly distributed across the arena during testing. Video recordings were taken and analyzed using Biobserve Viewer III (Biobserve GmbH, Germany). A virtual square of equal distance from the periphery (36 \times 36 cm) was defined as the “central zone” in order to determine the number of entries, and time (s) spent in the central zone. Distance moved in the outer and central zones (cm), number of entries and time spent in the central zone were registered. *Elevated Plus Maze:* The elevated plus maze was constructed from black opaque acrylic with white lining on the floor, each arm measuring 30 \times 5 cm and the central platform 5 \times 5 cm. One set of arms, opposing one another, were enclosed completely by a wall of opaque acrylic, 15 cm high, while the other set was open with a ledge of 0.5 cm either side of the arms. The open arms were brightly lit (100 lx). The maze was elevated 50 cm from the ground on a transparent acrylic stand. Each mouse was placed on the central platform, facing towards a closed arm, and allowed to freely explore the maze for 5 min. Biobserve Viewer III tracking software (Biobserve GmbH, Germany) was used to record locomotor activity during the test (distance moved in the open and closed arms), and the number of entries into the closed and open arms and time spent in them. An arm entry was counted when 2 paws had entered an arm, and an arm exit

was determined when 2 paws had left the arm. *Light dark box:* For the light-dark test, a box of white acrylic was used (50 \times 50 cm). The box was partitioned with a white acrylic wall, so that one-third of the total area was dark (“dark chamber”). The remaining two-thirds were brightly lit (100 lx) with white light, which served as the “light chamber.” A small entry door within the partition (5 \times 7 cm), allowed mice to move freely between chambers. Each mouse was placed into the dark chamber facing the end wall parallel to the partition. Activity was recorded for the following 5 min using Biobserve Viewer III (Biobserve GmbH, Germany). Locomotor activity (distance moved in cm) and time (s) in the dark and light chambers, and latent period of first entrance into the light chamber were measured. A single transition was counted when 2 paws had entered a chamber. *Novelty suppressed feeding:* Animals were deprived from food for 24 h before NSF test. After food deprivation, each mouse was put in the corner of a square white acrylic arena (50 \times 50 \times 50 cm), facing an outer wall. White light of 100 lx was evenly distributed across the arena during testing. A piece of food was placed in the center of the arena. Video recordings were taken and analyzed using Biobserve Viewer III (Biobserve GmbH, Germany). The time (s) before a mouse began eating after the fasting period (24 h) and the distance moved before eating were registered. *Forced swim test:* For the forced-swim test, each mouse was placed into a glass transparent cylinder (17 cm diameter, 18 cm height) filled with water (12 cm, 25 $^{\circ}\text{C}$) for 15 min. Then an animal was returned to the home cage. After 24 h, mice were again placed in this cylinder with water for 5 min. The latency of first floating, and total floating time during days 1 and 2 were recorded manually. *Sucrose preference test:* Animals were single housed and had access to 2 bottles with water 7 days before the SPT. At day 8, water in 1 bottle was replaced by 2% sucrose solution, and the position of bottles with water and sucrose solution was changed daily during the next 4 days. The weight of animals was measured before and after the test, volume of water and sucrose solution was estimated daily. Sucrose preference in % of drunken fluid was calculated.

Emotional behavior—pharmacology

In order to test the effects of an acute pharmacological inhibition of NSM on the emotional state, naïve male C57Bl6 mice ($n=8/\text{group}$) were continuously administered with a selective NSM inhibitor GW4869 (Sigma) in the dose of 2 mg/kg/day via Alzet osmotic mini pumps as described above. After the implantation, the animals were single housed and left for recovery for 6 days. Thereafter, the animals were tested in a battery of behavioral tests including the OF, elevated plus maze, and NSF test as described above. Mice were returned to their home cages at the end of each test and allowed to recover for at least 1 day before further testing (Müller et al. 2017; Kalinichenko et al. 2021).

Validation of emotional behavior in male rats

Thirty naïve male Wistar rats, aged 8–9 weeks, were purchased from Janvier (Le Genest St. Isle, France). Rats were grouped in 5 per cage and housed in Makrolon cages (Type IV) with well-controlled temperature and humidity conditions. All animals were given free access to water and food on a 12 h/12 h light–dark cycle (lights on at 19:00). They were allowed to adapt to the environment over 3 weeks and, then, handled for 5 min/rat/day for 3 consecutive days prior to experimentation. All experiments were carried out in accordance with the National Institutes of Health guidelines for the humane treatment of animals and the European Communities Council Directive (86/609/EEC) and approved by the local governmental commission for animal health.

Elevated plus maze: A plus-shaped maze was fixed 50 cm high from the floor and contained two open arms (50 × 10 cm), 2 closed arm with surrounding walls (50 × 10 × 40 cm) and a center area (10 × 10 cm). Each arm was installed in each edge of the center area in order (open arm, closed arm, open arm, closed arm). The illuminations (open arm: 3 lx, closed arm: 14 lx) were followed by the previous protocol (Pum et al. 2009; Wang et al. 2019). **Novelty suppressed feeding:** An unfamiliar OF (55 × 55 × 45 cm), evenly illuminated (corners and center ~6 lx), was utilized. A round, transparent dish ($d=7$ cm) was placed in the center of the OF containing a thin black rubber to prevent the reflection under lab chow. The apparatus was cleaned with 70% ethanol prior to each trial to eliminate the possible odor cues from previous animals. Twenty-four hours before the NSF, rats were food-deprived with free water access. The dish containing 2–3 lab chow was placed in the center of the unfamiliar OF before trial start. An animal was placed in one of the corners of the apparatus and allowed to explore freely for a maximum of 15 min, if they did not consume any lab chow. As soon as they were observed to eat, or the 15 min time limit was reached, the trial was terminated immediately. They were removed from the OF and put back to their home cage. Latencies to begin eating (s) and the locomotor activity (cm) were recorded automatically by EthoVision. After completion of behavioral testing, rats were anesthetized with carbon dioxide. Brain DH tissue was collected in 1.3 mL EDTA vial (Sarstedt), and centrifuged at 3,000 RPM at the room temperature for 5 min. NSM activity was analyzed in these samples as described previously (Mühle and Kornhuber 2017; Kalinichenko et al. 2021).

Emotional behavior after alcohol exposure

Alcohol drinking was established in naïve male fro and WT mice (fro: $n=8/7$; WT: $n=8/8$) using a 2-bottle free-choice drinking paradigm as described above. After 12 days drinking of 16 vol.% alcohol (control: water only), animals were tested in a battery of behavioral tests including OF, elevated plus maze, NSF, and forced swim test (FST), as described above. The mice continued drinking 16 vol.% alcohol in their home cages throughout

the whole testing (Müller et al. 2017; Kalinichenko et al. 2021).

Mouse MRI and CT

Magnetic resonance imaging (MRI) was used to investigate the effects of alcohol on the volume of DH, insular cortex, ventral and dorsal striatum, amygdala, and cerebellum in animals with NSM hypoactivity. Alcohol- or water-drinking was established in naïve male fro and WT mice (fro: $n=8/8$; WT: $n=8/8$) using a 2-bottle free-choice drinking paradigm as described above (Müller et al. 2017; Kalinichenko et al. 2021). After 12 days drinking of 16 vol.% alcohol, animals were exposed to MRI (Mielenz et al. 2018). A small-animal MRI system (ClinScan 70/30, Bruker BioSpin MRI GmbH, Ettlingen, Germany) was used for image acquisition. Animals were anesthetized with isoflurane (1.5%) prior to the procedure. During the MRI scan, an animal monitoring system was used for surveillance of heart and lung functions. The body core temperature was kept constant during the procedure at 37 °C using a heated pad. The volume and the signal intensity of the structures given above were calculated by measuring the respective regions of interest using Chimaera's segmentation tool (Chimaera GmbH). The following T2 Turbo Spin Echo sequence was used: Time of acquisition 14:03 min, voxel size 0.078 × 0.078 × 0.4 mm, TE: 44 ms, TR: 5,660 ms, slice thickness 0.4 mm, 30 slices.

Using computed tomography (CT), bone density was determined in various osseous structures (skull, spine, femur, tibia, humerus, radius, and ulna) by assessing the Hounsfield Units (HU) of the respective bone. For acquisition, a whole-body protocol was performed on a dedicated micro CT scanner (Inveon, Siemens) with the following parameter: Projections 180, settle time 1,000 ms, pixel size 51 μm , voltage 80 kV, current 500 μA , exposure 1,100 ms.

Neurogenesis

The effects of alcohol on neurogenesis in the hippocampus was evaluated in male fro and WT mice (fro: $n=4/4$; WT: $n=4/4$). Alcohol- or water-drinking was established in naïve animals using a 2-bottle free-choice drinking paradigm as described above (Müller et al. 2017; Kalinichenko et al. 2021). After further 9 days drinking of 16 vol.% alcohol, animals were sacrificed and the brains were isolated. The following primary antibodies were used: rabbit anti-MCM2 (1:500, Cell Signaling Technologies), mouse anti-Nestin (1:500; Millipore) and guinea pig anti-DCX (1:250; Millipore). Primary antibodies were visualized with Fluorophore-conjugated secondary antibodies. Rabbit anti-488 (1:1,000; Jackson ImmunoResearch), mouse anti-Cy³ (1:1,000; Jackson ImmunoResearch) and guinea pig anti-Cy³ (1:1,000; Jackson ImmunoResearch) were used as secondary antibodies. Immunofluorescent stainings were performed on free-floating 40 μm thick brain sections. Slices were washed with tris-buffered saline (TBS) overnight. Sections were rinsed 2 times for 15 min with TBS, rinsed

once in blocking solution I (TBS with 10% normal donkey serum and 0.3% Triton-X-100) at room temperature for 1 h and incubated with primary antibodies in blocking solution I for 72 h at 4 °C. After rinsing 3 times for 15 min in TBS, sections were rinsed 1 h in blocking solution II (TBS with 3% FCS and 0.3% Triton-X-100) and incubated with secondary antibodies in blocking solution II at 4 °C overnight. After washing thoroughly in TBS, nuclei were stained with DAPI (Sigma), sections were washed 3 times with TBS for 15 min and mounted on coverslips with Prolong Gold (Thermo Fisher Scientific Invitrogen).

All quantifications were done in a blinded fashion. Stage-specific marker expression (Nestin, MCM2, DCX) were quantified on a fluorescence microscope (Imager.M2, Zeiss, Jena, Germany) with the Zen2 pro (blue edition) software (Zeiss, Jena, Germany) in 2 sections containing the dentate gyrus from 16 different animals (4 from each group). Images were taken with the 20× objective lens and were processed using Zen lite (blue edition) software (Zeiss, Jena, Germany) (Kalinichenko et al. 2021).

Oxidative stress

The effects of alcohol on the oxidative stress in the brain was evaluated in male fro and WT mice (fro: $n=6/6$; WT: $n=6/6$). Alcohol drinking was established in naïve animals using a 2-bottle free-choice drinking paradigm as described above. After 12 days drinking of 16 vol.% alcohol, animals were sacrificed and the brains were isolated. Frozen brain tissues were homogenized in a polyphosphate buffer solution (pH=7.5). Oxidative stress markers were determined using a commercial assay kits according to manufacture protocols. Superoxide dismutase (SOD) activity was measured using Superoxide Dismutase Assay Kit (706,002; Cayman Chemical, USA), which utilizes a tetrazolium salt for detection of superoxide radicals generated by xanthine oxidase and hypoxanthine. SOD activity was determined as the amount of enzyme ability that exhibit 50% dismutation of the superoxide radical and is expressed as [U] per mL of tissue homogenates [U/mL] (Müller et al. 2017). Catalase activity was measured using the Catalase Assay Kit (707,002; Cayman Chemical, USA), which utilizes the peroxidic function of catalase for the determination of enzyme activity. The method is based on the reaction of the enzyme with methanol in the presence of an optimal concentration of H_2O_2 . The formaldehyde produced is measured colorimetrically with 4-amino-3-hydrazino-5-mercapto-1,2,4-triazole. This chromogen specifically forms a bicyclic heterocycle with aldehydes, which upon oxidation changes from colorless to purple color. One unit is defined as the amount of enzyme that will cause the formation of 1 nmol of formaldehyde per minute at 25 °C [nmol/min/mL]. Lipid peroxidation was performed using Thiobarbituric Acid Reactive Substances (TBARS) Assay Kit (700,870; Cayman Chemical, USA). The measurement of TBARS is a well-established method for screening and monitoring lipid peroxidation.

The malondialdehyde (MDA), naturally occurring product of lipid peroxidation, and thiobarbituric acid (TBA) under high temperature (90–100 °C) and acidic conditions formed the MDA–TBA adduct measured colorimetrically at 540 nm. The data are calculated using a standard curve of different MDA concentrations and presented as MDA [μ M] (Smaga et al. 2012; Kalinichenko et al. 2021).

Lipidomics

Alcohol- or water-drinking was established in naïve male fro and WT mice using a 2-bottle free-choice drinking paradigm as described above (fro: $n=6/6$; WT: $n=6/6$). After 12 days drinking of 16 vol.% alcohol, animals were sacrificed and DH was isolated and immediately frozen on dry ice. Lipidomic profiling was performed using Ultra Performance Liquid Chromatography–Tandem Mass Spectrometry (UPLC–MS), at the Biomarkers Core Laboratory, at Columbia University Irving Institute for Clinical and Translational Research, New York City, NY, USA. Lipid extracts were prepared from flash frozen samples using a modified Bligh and Dyer method (Bligh and Dyer 1959), spiked with appropriate internal standards, and analyzed on a platform comprising Agilent 1260 Infinity HPLC integrated to Agilent 6490A QQQ mass spectrometer controlled by Masshunter v 7.0 (Agilent Technologies, Santa Clara, CA). Glycerophospholipids and sphingolipids were separated with normal-phase HPLC as described before (Chan et al. 2012). An Agilent Zorbax Rx-Sil column (2.1 × 100 mm, 1.8 μ m) maintained at 25 °C was used under the following conditions: mobile phase A (chloroform: methanol: ammonium hydroxide, 89.9:10:0.1, v/v) and mobile phase B (chloroform: methanol: water: ammonium hydroxide, 55:39:5.9:0.1, v/v); 95% A for 2 min, decreased linearly to 30% A over 18 min and further decreased to 25% A over 3 min, before returning to 95% over 2 min and held for 6 min. Separation of sterols and glycerolipids was carried out on a reverse phase Agilent Zorbax Eclipse XDB-C18 column (4.6 × 100 mm, 3.5 μ m) using an isocratic mobile phase, chloroform, methanol, 0.1 M ammonium acetate (25:25:1) at a flow rate of 300 μ L/min. Quantification of lipid species was conducted using multiple reaction monitoring (MRM) transitions (Hsu et al. 2004; Guan et al. 2007; Chan et al. 2012), under both positive and negative ionization modes in conjunction with referencing of appropriate internal standards: PA 14:0/14:0, PC 14:0/14:0, PE 14:0/14:0, PG 15:0/15:0, PI 17:0/20:4, PS 14:0/14:0, BMP 14:0/14:0, APG 14:0/14:0, LPC 17:0, LPE 14:0, LPI 13:0, Cer d18:1/17:0, SM d18:1/12:0, dhSM d18:0/12:0, GalCer d18:1/12:0, GluCer d18:1/12:0, LacCer d18:1/12:0, D7-cholesterol, CE 17:0, MG 17:0, 4ME 16:0 diether DG, D5-TG 16:0/18:0/16:0 (Avanti Polar Lipids, Alabaster, AL). Lipid levels for each sample were calculated by summing up the total number of moles of all lipid species measured by all 3 LC–MS methodologies, and then normalizing that total to mol %. The final data are presented as mean mol % with error bars showing mean \pm SD.

Osteocalcin—ELISA

Circulating levels of osteocalcin (bone Gla protein) were measured in the blood serum of naïve male fro and WT mice (fro: $n=9$; WT: $n=9$) using the LSBio sandwich ELISA kit (LS-F12227) according to manufacturer's recommendations.

Osteocalcin treatment

Recombinant mouse osteocalcin (Cusabio; MBS948782) in the dose of 0.03 $\mu\text{g}/\text{h}$ or vehicle were administered continuously to male C57Bl6 mice ($n=8/\text{group}$) via Alzet osmotic mini pumps (model 1004; 28 day delivery; DURECT Corporation). Mini pumps were filled with the solution of osteocalcin in 1 \times PBS and implanted into the lower back of animals under isoflurane anesthesia (Isoflurane; Baxter Germany GMBH; 5% induction, 2% maintenance). Control animals were implanted with vehicle-containing pumps. After the implantation, the animals were single housed with 2 water bottles and left for recovery for 6 days. Thereafter, the animals were tested in a battery of behavioral tests including the OF, elevated plus maze, and NSF as described above. Mice were returned to their home cages at the end of each test and allowed to recover for at least 1 day before further testing. Behaviors for all tests were recorded on videotape for subsequent scoring. After the last behavioral test, the animals were exposed to alcohol on the model of 2-bottle free-choice paradigm as mentioned above. The concentration of alcohol gradually increased from 2 to 16% every 2 days, the concentration of 16% was kept for 5 days. Then the animals were sacrificed by cervical dislocation (Kalinichenko et al. 2021).

Statistical analyses

Data were examined with 1- or 2-way analysis of variance (ANOVA), for repeated measures where appropriate. For single group and time point effects, preplanned comparisons were calculated using Bonferroni-corrected least significant difference (LSD)-tests or *t*-tests (Ramsey 1993). A *P*-value of ≤ 0.05 was considered indicative of statistical significance.

Results

Reduced NSM function enhances alcohol drinking

In order to test the role of NSM in voluntary alcohol consumption, we investigated heterozygous NSM knock out mice (fro; Aubin et al. 2005) in a 2-bottle-free choice alcohol consumption test. Animals had all the time the choice between alcohol (2–16 vol. %) or water (Mielenz et al. 2018; Müller et al. 2019). Male fro mice showed a significantly enhanced alcohol consumption compared to WT controls (2-way ANOVA, factor genotype: $F_{1,35}=4.3112$, $P=0.0452$; factor alcohol concentration: $F_{4,140}=178.7101$, $P<0.0001$; interaction: $F_{4,140}=2.1264$, $P=0.0807$). Preplanned comparisons yielded a significant difference at single doses for 8 vol.% ($P=0.0272$),

12 vol.% ($P=0.0093$), and 16 vol.% ($P=0.0355$) (Fig. 1a). Lack of NSM function had no significant effect on total fluid consumption in male mice (2-way ANOVA, factor genotype: $F_{1,35}=1.8867$, $P=0.1783$; factor alcohol concentration: $F_{4,140}=8.7073$, $P<0.0001$; interaction: $F_{4,140}=1.4655$, $P=0.2159$). Preplanned comparisons did not show significant difference at single dose level ($P>0.05$; Fig. 1b; Supplementary Fig. 1).

In order to test whether the NSM effect is an acute effect or depends on developmental lack of NSM function, we tested the effects of an acute pharmacological inhibition of NSM activity on alcohol drinking. Alcohol drinking was enhanced in male C57Bl6 mice in a 2-bottle free-choice drinking test by chronic treatment with the NSM inhibitor GW4869 (Airoola and Hannun 2013) administered by osmotic mini-pumps at a rate of 2 mg/kg/day (i.p.) during alcohol drinking at increasing concentrations (2-way ANOVA, factor treatment: $F_{1,14}=3.943$, $P=0.067$; factor alcohol concentration: $F_{4,56}=200.593$, $P<0.0001$; interaction: $F_{4,56}=0.975$, $P=0.428$). While alcohol consumption was enhanced at all concentrations, preplanned comparisons showed a significant effect only for 4 vol.% alcohol ($P<0.0001$) (Fig. 1c). No effect of the GW4869 treatment was observed on free water consumption in these animals (2-way ANOVA, factor treatment: $F_{1,14}=0.182$, $P=0.676$; factor alcohol concentration: $F_{4,56}=1.633$, $P=0.179$; interaction: $F_{4,56}=1.011$, $P=0.409$). Preplanned comparisons showed no significant difference on single days ($P>0.05$) (Fig. 1d; Supplementary Fig. 2). Together these findings suggest an inhibitory role of NSM on free-choice alcohol drinking in male mice.

Attenuated NSM function delays the establishment, but not retrieval of alcohol conditioned behavior

A major driver of alcohol addiction is the establishment and later retrieval of drug seeking behavior. We tested the establishment of an alcohol-induced CPP in fro mice (Huston et al. 2013; Easton, Lucchesi, Lourdusamy, et al. 2013). We found a delayed establishment of an alcohol CPP in male fro mice (Fig. 1e). A 2-way ANOVA confirmed the establishment of an alcohol CPP (factor time: $F_{3,51}=7.5728$, $P=0.0003$), but did not show an effect of genotype ($F_{1,17}=3.1790$, $P=0.0925$) or interaction ($F_{3,51}=1.7679$, $P=0.1650$). Preplanned comparisons showed a significant increase of time in the conditioning compartment in WT mice already at T1 ($P=0.0105$) and T3 ($P=0.0009$), while for fro mice only at T3 ($P=0.0225$). In males, acute locomotor effects of alcohol and conditioned hyperlocomotion were not altered by reduced NSM function (Fig. 1f; 2-way ANOVA; factor genotype: $F_{1,17}=0.0002$, $P=0.9893$, factor treatment day: $F_{6,102}=1.6301$, $P=0.1463$), interaction: $F_{6,102}=0.6979$, $P=0.6518$; preplanned comparisons: all $P>0.05$; Supplementary Fig. 3). Our previous studies did not reveal any memory impairments in male fro mice, which could determine the delayed establishment of an

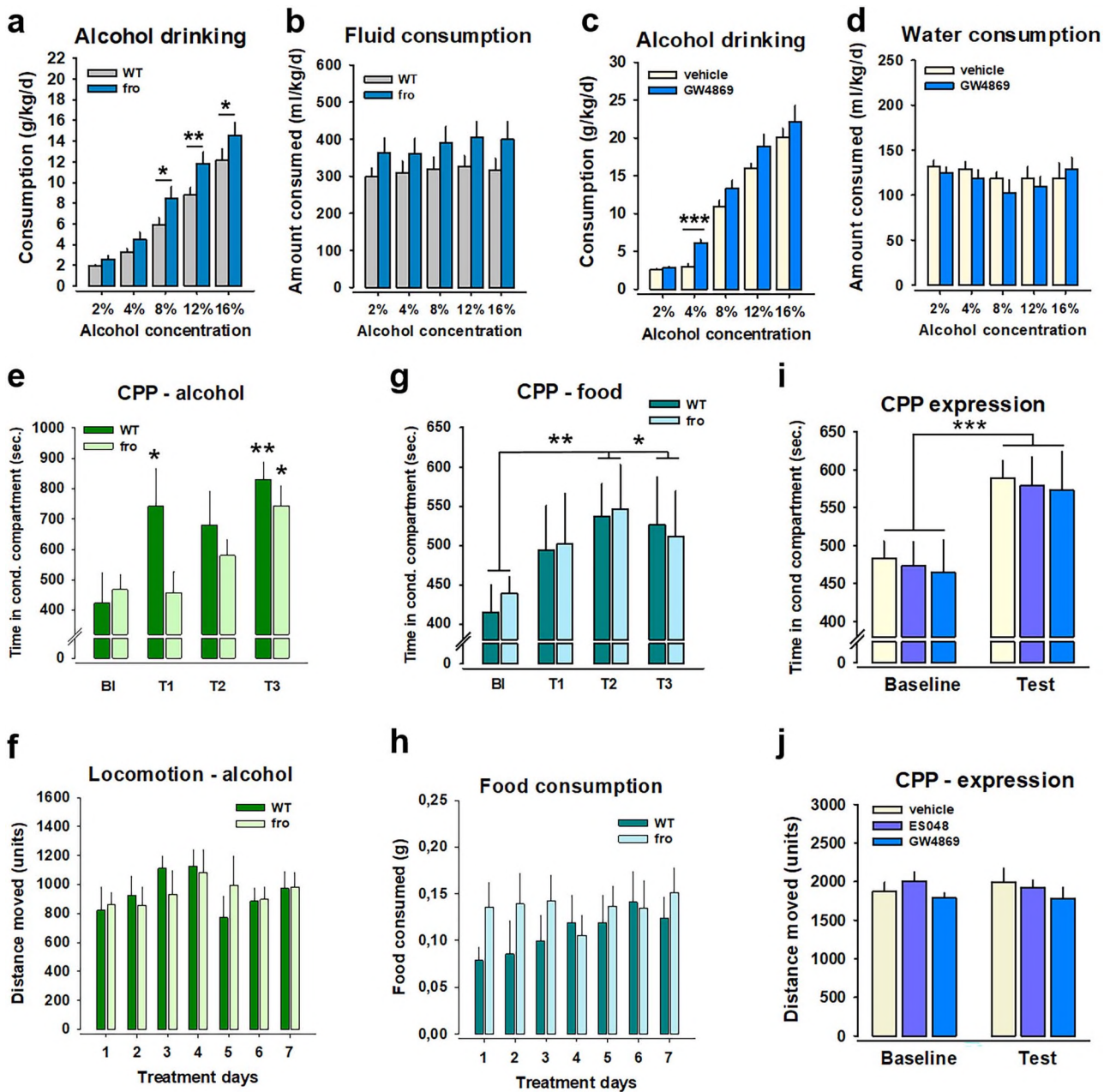


Fig. 1. Neutral sphingomyelinase determines alcohol consumption and conditioned rewarding effects in males. (a) Male mice with a heterozygous NSM-2 knock out (fro) show enhanced alcohol consumption in a 2-bottle free choice paradigm compared to WT controls. (b) Lack of NSM function did not significantly affect total fluid consumption in male mice. (c) Male fro mice show an increased alcohol consumption in a 2-bottle free choice paradigm after pharmacological NSM inhibition with the antagonist GW4869 compared to WT controls (d) inhibition of NSM has no effect on total fluid consumption in male mice. (e). Delayed establishment of alcohol CPP in male fro mice. Alcohol (2 g/kg; i.p.) was paired at 7 occasions with a conditioning (cond.) compartment. CPP was tested after 1 (T1), 3 (T2), and 7 (T3) conditioning and saline-pseudoconditioning trials (BI—Baseline). (f) No difference in acute or subchronic locomotor response to alcohol during conditioning procedure. (g) NSM is not involved in the establishment of the conditioned reinforcing effects of preferred food in males. (h) An initial preference of the food in fro mice fades with repeated exposure during conditioning. (i) NSM is not involved in the expression of the conditioned reinforcing effects of alcohol in male mice as the 2 NSM inhibitors GW4869 and ES048 applied before CPP retrieval, did not affect CPP expression. (j) No effect of NSM inhibition on locomotor activity during CPP expression in males ($P > 0.05$). Mean \pm SEM (* $P \leq 0.05$, ** $P \leq 0.01$, *** $P \leq 0.001$).

alcohol-induced CPP (Kalinichenko et al. 2021). Therefore, the observed delay appears to be alcohol-induced, but not based on a decline of memory.

In order to distinguish a role of NSM in the conditioned reinforcing effects between alcohol and a natural reinforcer, we tested mice also for food-induced CPP, using a highly palatable food that can induce a CPP also

in satiated mice (Hess et al. 2019). While food worked well as a natural reinforcer in male mice, reduced NSM activity had no effect on CPP establishment (Fig. 1g). A 2-way ANOVA confirmed the establishment of a food CPP (factor time: $F_{3,51} = 3.5621$, $P = 0.0204$), but did not show an effect of genotype ($F_{1,17} = 0.0141$, $P = 0.9069$) or interaction ($F_{3,51} = 0.0933$, $P = 0.9633$). Post-hoc test

vs. BL confirmed an overall increase in the time in the conditioning compartment at T2 ($P=0.0099$) and T3 ($P=0.05$). Food consumption did not differ significantly between male fro and WT mice ($P>0.05$) (Fig. 1h; Supplementary Figs. 4–6).

The expression of a previously established alcohol CPP was not affected by NSM antagonist treatment with ES048 or GW4869 in male mice (Fig. 1i) (2-way ANOVA; factor treatment: $F_{2,23}=0.0654$, $P=0.9368$, factor time: $F_{1,23}=49.4246$, $P<0.0001$, interaction: $F_{2,23}=0.0025$, $P=0.9974$; preplanned comparisons between treatment groups: all $P>0.05$). Neither did these treatments affect locomotor activity ($P>0.05$; Fig. 1j; Supplementary Figs. 7–9).

Altogether, these findings suggest that NSM is necessary to establish, but not to retrieve the conditioned reinforcing effects of alcohol. It is not involved in the reinforcing action of natural reinforcers.

Sex-specific monoamine transmitter control by NSM

Crucial mediators of the reinforcing action and addiction development of alcohol are the DA- and 5-HT-systems and their adaptations after chronic drug exposure (Spanagel 2009; Müller and Homberg 2015). Previously, a strong interaction of acid sphingomyelinase with brain monoamine tissue levels and alcohol responses were reported (Müller et al. 2017; Kalinichenko et al. 2019). We used in-vivo microdialysis in freely moving mice to test extracellular monoamine levels and responses to an acute alcohol challenge. Reduced NSM activity led to a significant reduction of basal extracellular DA levels in the DH ($t=-2.067$, $P=0.045$), and an increase in 5-HT levels in the Nac ($t=2.160$, $P=0.045$) (Fig. 2a–g). The DA-response to alcohol was enhanced in the Nac (2-way ANOVA; factor genotype: $F_{1,13}=0.618$, $P=0.446$, factor time: $F_{6,78}=3.753$, $P=0.002$, interaction: $F_{6,78}=2.689$, $P=0.02$; preplanned comparisons vs. baseline (BL), fro: 60 min: $P=0.008$; WT, 120 min: $P=0.017$; Fig. 2b). Alcohol caused a small, but nonsignificant increase in DH DA levels in fro and WT mice ($P>0.05$) (Fig. 2d). Alcohol had no effect on Nac 5-HT levels ($P>0.05$; Fig. 2f), but enhanced DH 5-HT levels in male WT mice. This effect in the DH was attenuated in fro mice (2-way ANOVA; factor genotype: $F_{1,12}=2.416$, $P=0.146$, factor time: $F_{6,72}=1.524$, $P=0.183$, interaction: $F_{6,72}=0.613$, $P=0.719$; preplanned comparisons vs. BL, WT, 20 min: $P=0.046$, 80 min: $P=0.047$; fro, $P>0.05$; Fig. 2h).

Sphingomyelinase treatment inhibited 5-HT uptake in synaptosomes from DH ($P<0.01$) and vStr ($P<0.05$), but not from VH ($P>0.05$), of male mice (Fig. 2i). This may explain the increase in Nac extracellular 5-HT levels in fro mice. Altogether, this shows a functional role of NSM in the regulation of basal monoaminergic activity and in the DA- and 5-HT responses to alcohol. In particular, the enhanced Nac DA response may suggest stronger pharmacological reinforcing action of alcohol in

male fro mice, and, thus, support an increased alcohol consumption.

NSM regulation of monoamine signaling

Synaptic throughput also requires receptor and transport mechanisms (Amato et al. 2020). Sphingolipid microdomains were shown to shape monoamine receptor conformation and function as well as transporter efficacy (Magnani et al. 2004; Fantini and Barrantes 2009; Bjork et al. 2010; Kim, Ahn, Jeon, et al. 2010a). Here, we measured mRNA expression levels of major receptors and transporters involved in dopaminergic and serotonergic signaling in the vStr of male mice. No differences were observed between fro and WT mice ($P>0.05$; Fig. 2j–q). Alcohol consumption increased vStr mRNA expression of DAT ($P=0.004$) and SERT ($P=0.02$), as well as of the 5-HT_{1A}- ($P=0.011$) and 5-HT_{2C}-receptors ($P=0.011$), in WT mice. After alcohol consumption, there emerged a difference in the expression of DA D1 ($P=0.027$) receptors and for DAT ($P=0.016$), as well as for 5-HT_{1A}- ($P=0.014$) and 5-HT_{2C}-receptors ($P=0.026$), and for SERT expression ($P=0.015$) between fro and WT mice (Fig. 2j–q). These findings suggest that a reduction in NSM function attenuates susceptibility to neuroplastic changes after chronic alcohol drinking in males.

NSM is a key regulator of emotional state

A human genetic study suggested an association of natural variability in SMPD3 and emotional behavior for male and female individuals (Kalinichenko et al. 2021). Here we tested in male mice how a reduced NSM activity would affect depression- and anxiety-like behavior (Müller et al. 2017; Mielenz et al. 2018). Male fro mice showed enhanced depression-like behavior in the NSF test compared to WT (Fig. 3a). This difference was eliminated when animals were stressed by corticosterone drinking, which caused by itself an increase in depression-like behavior (2-way ANOVA; factor genotype: $F_{1,37}=0.7246$, $P=0.4001$, factor stress: $F_{1,37}=10.7377$, $P=0.0023$, interaction: $F_{1,37}=0.0336$, $P=0.8554$). Preplanned comparisons confirmed more depression-like behavior in fro animals under the no-stress condition ($t=1.7789$, $P=0.0471$), but not under stress ($P>0.05$). Male fro mice showed enhanced depression-like behavior in the FST (Fig. 3b). This difference was eliminated by stress, which caused by itself an increase in depression-like behavior (2-way ANOVA; factor genotype: $F_{1,33}=0.7713$, $P=0.3861$, factor stress: $F_{1,33}=2.4461$, $P=0.1273$, interaction: $F_{1,33}=0.7097$, $P=0.4056$). Preplanned comparisons confirmed more depression-like behavior in fro animals under no-stress conditions ($t=1.8615$, $P=0.0391$), but not under stress ($P>0.05$). There was no overall effect on hedonic tone as measured in the SPT (Fig. 3c; 3-way ANOVA; factor genotype: $F_{1,38}=0.9411$, $P=0.9411$, factor time: $F_{4,152}=24.7202$, $P<0.0001$, factor stress: $F_{1,38}=0.0174$, $P=0.8958$; all interactions: $P>0.05$). Preplanned comparisons for single days showed enhanced sucrose preference for fro mice under stress on days

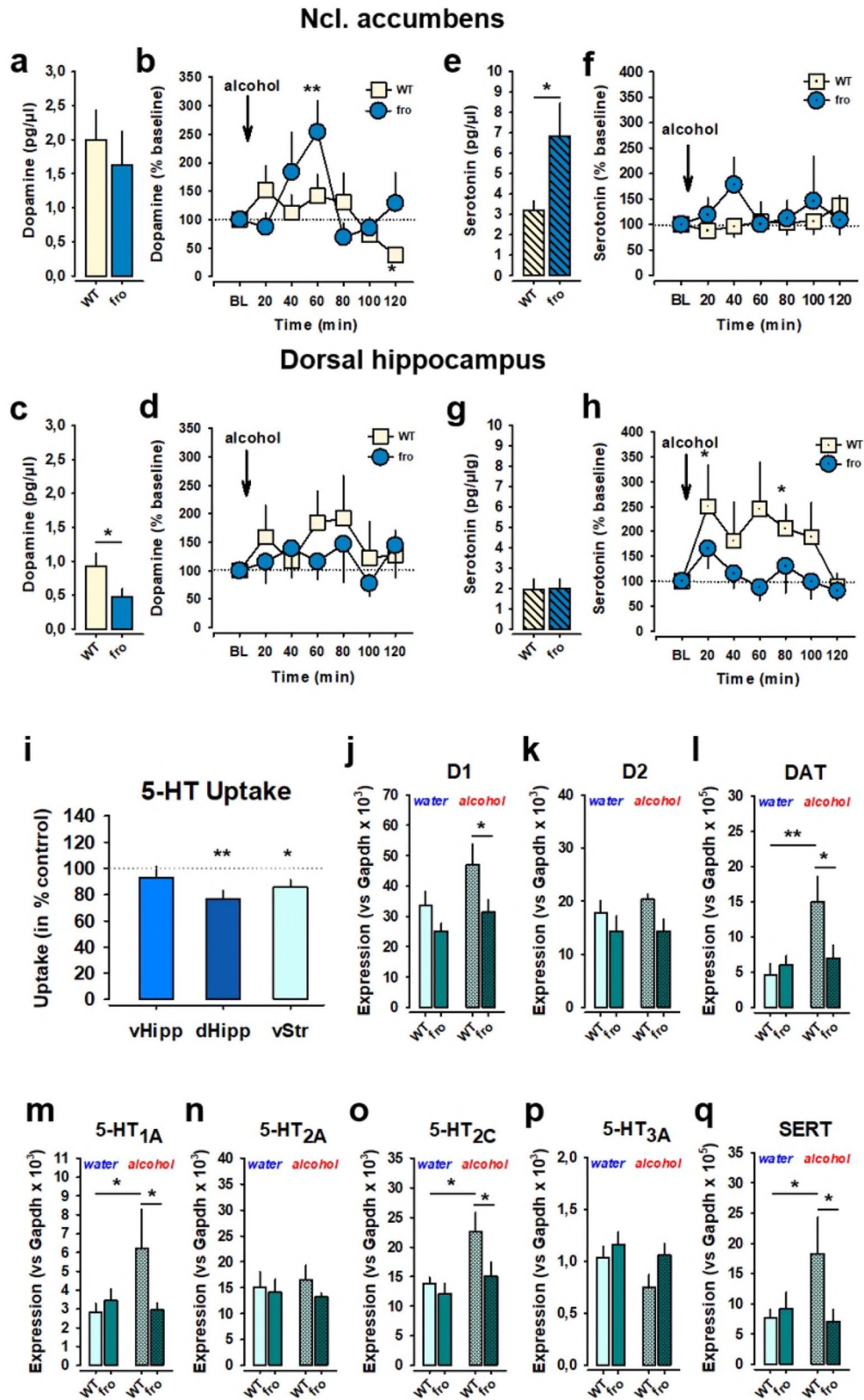


Fig. 2. Neutral sphingomyelinase controls acute and chronic effects of alcohol on monoaminergic signaling in the brain. (a–h) Heterozygous knock out of NSM affects basal extracellular dopamine and serotonin activity in the nucleus accumbens (Nac) and DH of male mice. An alcohol injection (2 g/kg, i.p.) enhanced extracellular dopamine (DA) and serotonin (5-HT) activity in the Nac and DH of WT mice. The DA increase in the Nac was enhanced, but the 5-HT increase in the DH was attenuated in fro mice (values are shown as percent baseline (BL), taken as 100%). (i) Sphingomyelinase treatment inhibits 5-HT uptake in synaptosomes from ventral hippocampus (vHipp), dorsal hippocampus (dHipp), and ventral striatum (vStr) of male mice. Pretreatment with 100 mU/mL bacterial sphingomyelinase BSM for 60 min. Values are expressed as percent of control (mean \pm SEM). Control levels (100%) are indicated by dotted line (* $P \leq 0.05$, ** $P \leq 0.01$, one sample t-test against theoretical mean of 100%). vStr mRNA expression after chronic alcohol or water drinking in male mice for the (j) DA D1-receptor, (k) DA D2-receptor, (l) the DA transporter (DAT), (m) the 5-HT_{1A}-receptor, (n) the 5-HT_{2A}-receptor, (o) the 5-HT_{2C}-receptor, (p) the 5-HT_{3A}-receptor, and (q) the 5-HT transporter (SERT). All results show mean \pm SEM (* $P \leq 0.05$, ** $P \leq 0.01$, *** $P \leq 0.001$).

3 ($P=0.0330$) and 5 ($P=0.0367$). Male fro mice showed enhanced anxiety-related behavior in the light dark box test (LDB) test (Fig. 3d; white compartment time, 2-way ANOVA; factor genotype: $F_{1,38}=3.3263$, $P=0.076$, factor stress: $F_{1,38}=2.6236$, $P=0.1135$, interaction: $F_{1,38}=0.2728$, $P=0.6045$; preplanned comparison for no-stress: $t=-1.868$, $P=0.0391$; dark compartment time; 2-way ANOVA; factor genotype: $F_{1,38}=3.335$, $P=0.0757$, factor stress: $F_{1,38}=2.715$, $P=0.1076$, interaction: $F_{1,38}=0.274$, $P=0.6036$; preplanned comparison for no-stress: $t=1.869$, $P=0.0389$). In the elevated plus maze test (EPM) test, fro mice showed more anxiety-like behavior than WT mice, a difference also eliminated by the effects of stress (Fig. 3e; 2-way ANOVA; factor genotype: $F_{1,37}=0.8460$, $P=0.3636$, factor stress: $F_{1,37}=17.5239$, $P=0.0002$, interaction: $F_{1,37}=0.0153$, $P=0.9021$; preplanned comparison for no-stress: $P=0.0029$). Also the OF test revealed an increase in anxiety-related behavior in fro mice, which was, however, not stress sensitive (Fig. 3f; 2-way ANOVA; factor genotype: $F_{1,40}=4.9183$, $P=4.9183$, factor stress: $F_{1,40}=0.5729$, $P=0.4535$, interaction: $F_{1,40}=0.0773$, $P=0.7824$; preplanned comparison for no-stress: $t=-2.3542$, $P=0.0151$; Supplementary Figs. 10–13).

A pharmacological inhibition of NSM activity with GW4869 in naive male mice confirmed an increase in depression-like behavior in the NSF test ($t=-1.779$, $P=0.05$; Fig. 3g), but had no effect on anxiety-like behavior in the EPM ($P>0.05$; Fig. 3h) and OF test ($P>0.05$; Fig. 3i). Neither did it affect locomotor activity (Supplementary Fig. 14). This relationship could be confirmed in a study of naïve male rats where we investigated brain NSM activity in the DH and used it as a predictor for depressive-like behavior. Results suggested that animals with low NSM activity in the DH after a median split ($t=5965$, $P<0.0001$; Fig. 3j) show significantly more depression-like behavior in the NSF test ($t=-2067$, $P=0.05$; Fig. 3k), but not more anxiety-like behavior in the EPM test ($P>0.05$; Fig. 3l). Altogether, these findings suggest a strong depressogenic and partial anxiogenic effect resulting from reduced NSM activity. Thereby, NSM activity in the DH may serve as a specific predictor for depression-like behavior.

Brain area volumes are controlled by NSM

After observing strong effects of NSM on drug rewarded and emotional behavior, which mainly arise from a developmental origin, we tested structural neuroanatomy of male fro mice after chronic consumption of alcohol or water using MRI (Mielenz et al. 2018; Müller et al. 2019). This analysis revealed that fro mice show a significantly reduced volume of the DH (2-way ANOVA; factor genotype: $F_{1,27}=14.591$, $P=0.001$, factor alcohol: $F_{1,27}=14.862$, $P=0.001$, interaction: $F_{1,27}=0.345$, $P=0.562$; preplanned comparisons, water: fro vs. WT, $P=0.004$; alcohol: fro vs. WT, $P=0.033$; Fig. 4a), the vStr (2-way ANOVA; factor genotype: $F_{1,28}=3.420$,

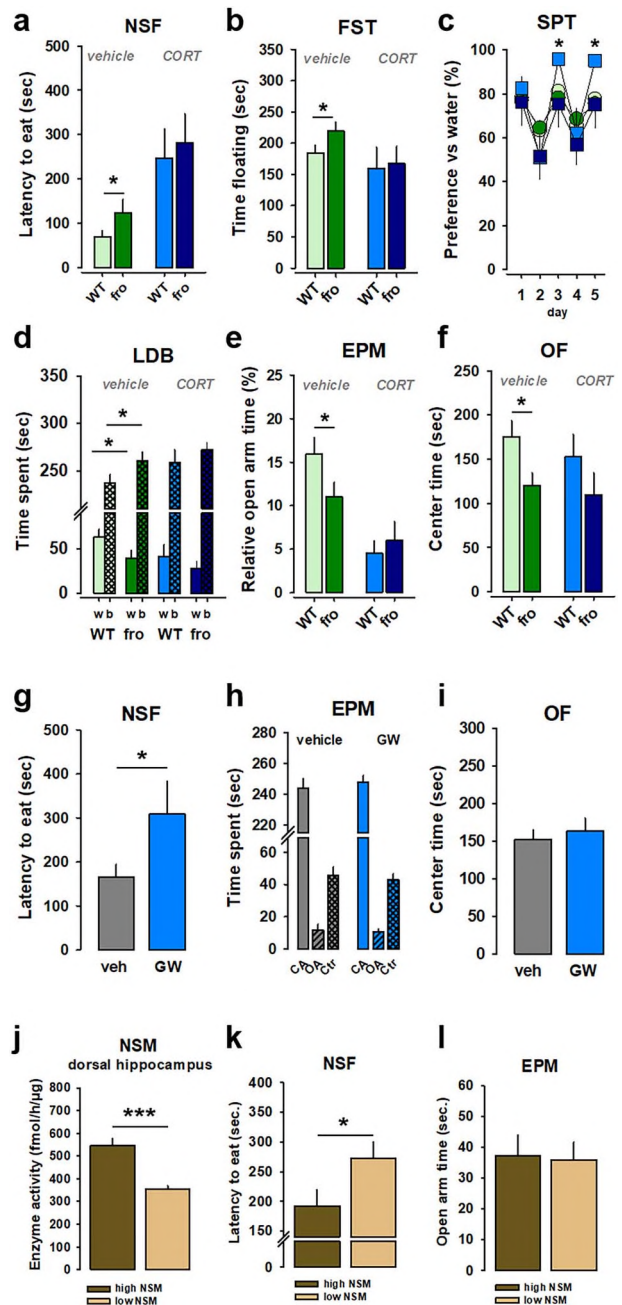


Fig. 3. NSM controls depression-like and anxiety-like behavior in males. Emotional behavior of male mice with heterozygous NSM knock out (fro) in (a) the NSF, (b) the FST, (c) the SPT, (d) the LDB, (e) the EPM, and (f) in the OF. (g) Pharmacological NSM inhibition in naive male mice with GW4869 (GW) enhances depression-like behavior in the NSF test, but has no effect on anxiety-like behavior in (h) the EPM, or (i) OF test. A sample of naïve male rats was analyzed for emotional behavior and NSM activity in the dorsal hippocampus. (j) A median split of this sample by NSM activity yielded a high and a low NSM activity group, which differed significantly in NSM activity. (k) Naturally low NSM activity predicts enhanced depression-like behavior in the NSF test, but (l) no anxiety-related behavior in the EPM test. All results show mean \pm SEM (* $P \leq 0.05$, ** $P \leq 0.01$, *** $P \leq 0.001$).

$P=0.075$, factor alcohol: $F_{1,28}=0.902$, $P=0.350$, interaction: $F_{1,28}=2.410$, $P=0.132$; preplanned comparisons, water: fro vs. WT, $P=0.023$; alcohol: fro vs. WT, $P=0.835$; Fig. 4c), and the cerebellum (2-way ANOVA; factor genotype: $F_{1,28}=2.857$, $P=0.102$, factor alcohol: $F_{1,28}=1.496$,

$P = 0.231$, interaction: $F_{1,28} = 1.325$, $P = 0.259$; preplanned comparisons, water: fro vs. WT, $P = 0.05$; alcohol: fro vs. WT, $P = 0.706$; Fig. 4f). No effects were found in other structures, such as the insular cortex, dorsal striatum, or amygdala ($P > 0.05$; Fig. 4b, d, e). As these areas are involved in emotional behavior (Gulbins et al. 2013, 2018) and alcohol abuse (Krishnan and Nestler 2008; Müller et al. 2017), attenuated processing capacity may partly explain the enhanced depression- and anxiety-levels in the male fro mice. Voluntary alcohol drinking for 46 days decreased the DH volume, but maintained genotype differences. This is in line with previous reports of hippocampal cell loss in males after prolonged alcohol consumption (Walker et al. 1980). In contrast, alcohol consumption enhanced vStr volume in male fro mice up to the level of WT mice.

Altogether, morphological analysis suggests that NSM effects on emotional behavior and alcohol drinking may be mediated by its role in brain development. Significant deficits in particular in the DH and vStr may be the base for reduced control of these behaviors in adult males.

NSM effects on hippocampal neurogenesis

As the DH emerged as a developmental focus of NSM activity, we tested how NSM controls hippocampal neurogenesis (Zhang and Jiao 2015). A reduction of NSM activity led to an increase in neural stem- and early-progenitor cells (Fig. 4g; water: $P < 0.05$; alcohol: $P < 0.05$), which, however, did not translate into enhanced number of proliferating cells (Fig. 4h), activated stem cells (Fig. 4i), or newborn neurons and neuroblasts (Fig. 4j) ($P > 0.05$). Chronic and binge alcohol exposure has been shown to reduce hippocampal cell proliferation and neurogenesis in male rats (Nixon and Crews 2002; He et al. 2005) and humans (Le Maitre et al. 2018). However, the current voluntary alcohol drinking scheme did not affect neurogenesis to such an extent. Accordingly, NSM effects on DH neurogenesis may not account for the reduced DH volume in male fro mice.

NSM control of oxidative stress

Brain area volume and functional circuit efficacy may also be controlled by regional oxidative stress, as there is a close interaction of sphingolipids with the regulation of oxidative stress (Stranahan et al. 2011). Oxidative stress, in turn, controls NSM phosphorylation (Filosto et al. 2010). Chronic voluntary alcohol consumption attenuated protective superoxide dismutase (SOD) activity in the DH of fro mice (Fig. 4k). This effect was eliminated by chronic alcohol consumption (2-way-ANOVA; factor: genotype: $F_{1,20} = 4.686$, $P = 0.0426$; factor: treatment: $F_{1,20} = 2.021$, $P = 0.1705$; interaction: $F_{1,20} = 3.069$, $P = 0.0951$; preplanned comparison, water: fro vs. WT: $P < 0.0236$). Catalase activity and lipid peroxidation, in contrast, were not affected ($P > 0.05$; Fig. 4l and m). These findings may suggest that a reduction in protective SOD activity

may contribute to volume loss in this region. However, it may not account for further decline after alcohol consumption.

NSM controls lipidome adaptations to alcohol

Chronic alcohol consumption is known to lead to large-scale adaptations in brain protein expression, which has direct effects on behavior. Addiction-related behaviors become established, but also virtually all other behaviors are altered. However, little is known about the effects on the lipidome, which can be crucial for the control of the emotional state and behavior (Oliveira et al. 2016). Here we investigated alterations in the lipidome after voluntary alcohol drinking and the role of the NSM. In male mice, chronic alcohol drinking led to a significant decline of triacylglycerol (TG), dihydro-shingomyeline (dhSM), globotriaosylceramide (GB3), bis(monoacyl)glycerol (BMP), lysophosphatidylethanolamine (LPE), and lysophosphatidylinositol (LPI) in the Nac (Fig. 5a). Reduced NSM activity alone enhanced only dhSM levels. However, it rendered the organism much more susceptible to alcohol effects on the lipidome, as now 20 of the 34 investigated lipid families were dysregulated in fro mice drinking alcohol. All were down-regulated, except monohexosylceramide (MhCer), which was up-regulated. Those included sphingomyelin (SM), the NSM substrate, but not ceramide (Cer), the catalysis product, when whole families were considered (Fig. 5b). However, a SM- and Cer-species analysis revealed a significant decline of Cer 16:0 after alcohol alone, which was prevented in fro mice (Fig. 5c). NSM was shown to control Cer generation in the brain (Tabatadze et al. 2010; Airola et al. 2017), which crucially shapes neuronal cell membrane structure and function (Hannun and Obeid 2008; van Meer et al. 2008). In this study, reduced NSM activity alone decreased Cer 22:0 levels and sensitized for reducing effects of alcohol on many Cer species of which Cer 20:1, Cer 22:1, and Cer 24:0 effects reached statistical significance. Chronic alcohol consumption alone reduced local Nac levels of virtually all SM species, which was significant for SM 22:0, SM 24:0, SM 24:1, SM 26:0, and SM 26:1 (Fig. 5d). Reduced NSM activity had no significant effects on local SM species in the Nac, but largely potentiated alcohol's declining effects in a way that all 12 detectable SM species were declined in fro mice after alcohol drinking. A strong potentiation of alcohol-induced increase by reduced NSM activity was also seen in 22 of the 24 detectable MhCer species, and a potentiation of the decrease in 5 of the 24 detectable lactosylceramide (LacCer) species (Supplementary Figs. 15–18). Together, these findings suggest that reduced NSM activity enhances lipidomic sensitivity for chronic alcohol effects.

No alcohol use for self-management of emotion in fro mice

Aversive mental states are self-managed with alcohol in humans (Müller et al. 2021) and mice (Müller et al. 2017;

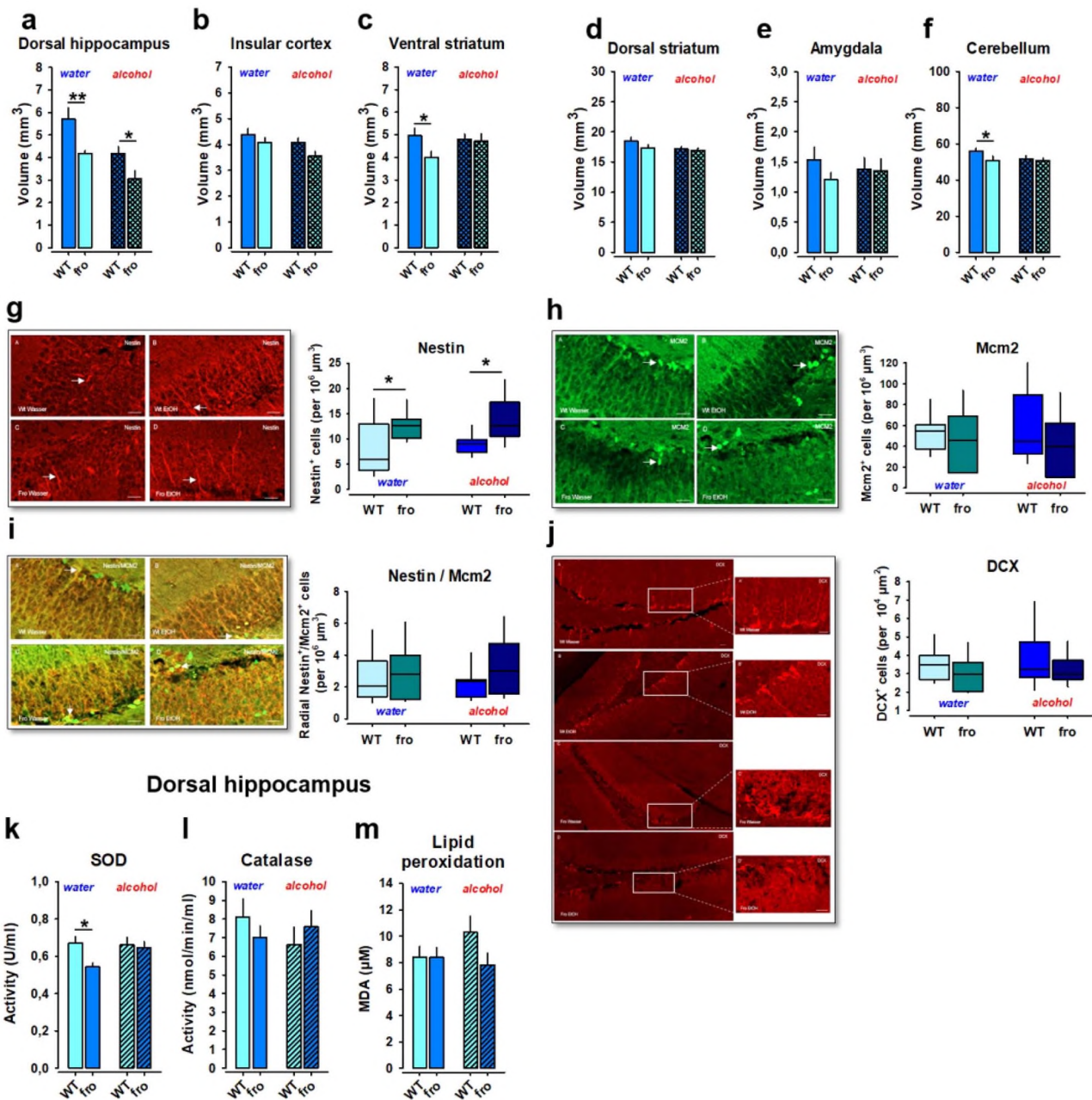


Fig. 4. Reduced NSM activity during development impairs brain area development in males. (a–f) In male mice with heterozygous NSM knock out (fro), brain area volume was significantly reduced in the dorsal hippocampus (DH), ventral striatum (vStr), and cerebellum. Voluntary alcohol drinking for 46 days (2–16 vol.%) reduced DH size in fro and WT mice, but had no effect on other brain regions. All results show mean \pm SEM (* $P \leq 0.05$, ** $P \leq 0.01$, *** $P \leq 0.001$). Effects of reduced NSM activity and alcohol drinking on dorsal hippocampus neurogenesis in mice. Representative photomicrographs of male fro and WT mice stained for (g) nestin, (h) Mcm2, (i) nestin/Mcm2, and (j) doublecortin (DCX) (bar = 20 μ m). (k) Lack of NSM function had a significant effect on oxidative stress in the DH of male mice. SOD was significantly reduced in male fro mice. Alcohol drinking had no effect on SOD activity in fro or WT mice. There was no effect of NSM or alcohol on (l) catalase activity or (m) lipid peroxidation in the DH of male mice ($P > 0.05$). All results show mean \pm SEM (* $P \leq 0.05$, ** $P \leq 0.01$, *** $P \leq 0.001$).

Müller and Kornhuber 2017). Here we tested whether voluntary self-titrated alcohol drinking can reverse the adverse emotional phenotype in male fro mice. Voluntary alcohol drinking enhanced anxiety-, but not depression-like behaviors in WT mice. However, it had little effect in fro mice ($P > 0.05$; Supplementary Figs. 19–22). These findings suggest that the NSM may not be involved in the self-management of emotional states by voluntary alcohol drinking.

Peripheral action of NSM—role of the bone–brain signaling pathway

In a human association study, naturally occurring polymorphisms in the NSM coding gene *SMPD3* were not only associated with alcohol consumption and emotional state, but also with bone integrity (Kalinichenko et al. 2021). An important role of NSM in bone mineralization is known from fragile oss syndrome, a natural occurring mutation with a homozygous *SMPD3* deletion resulting

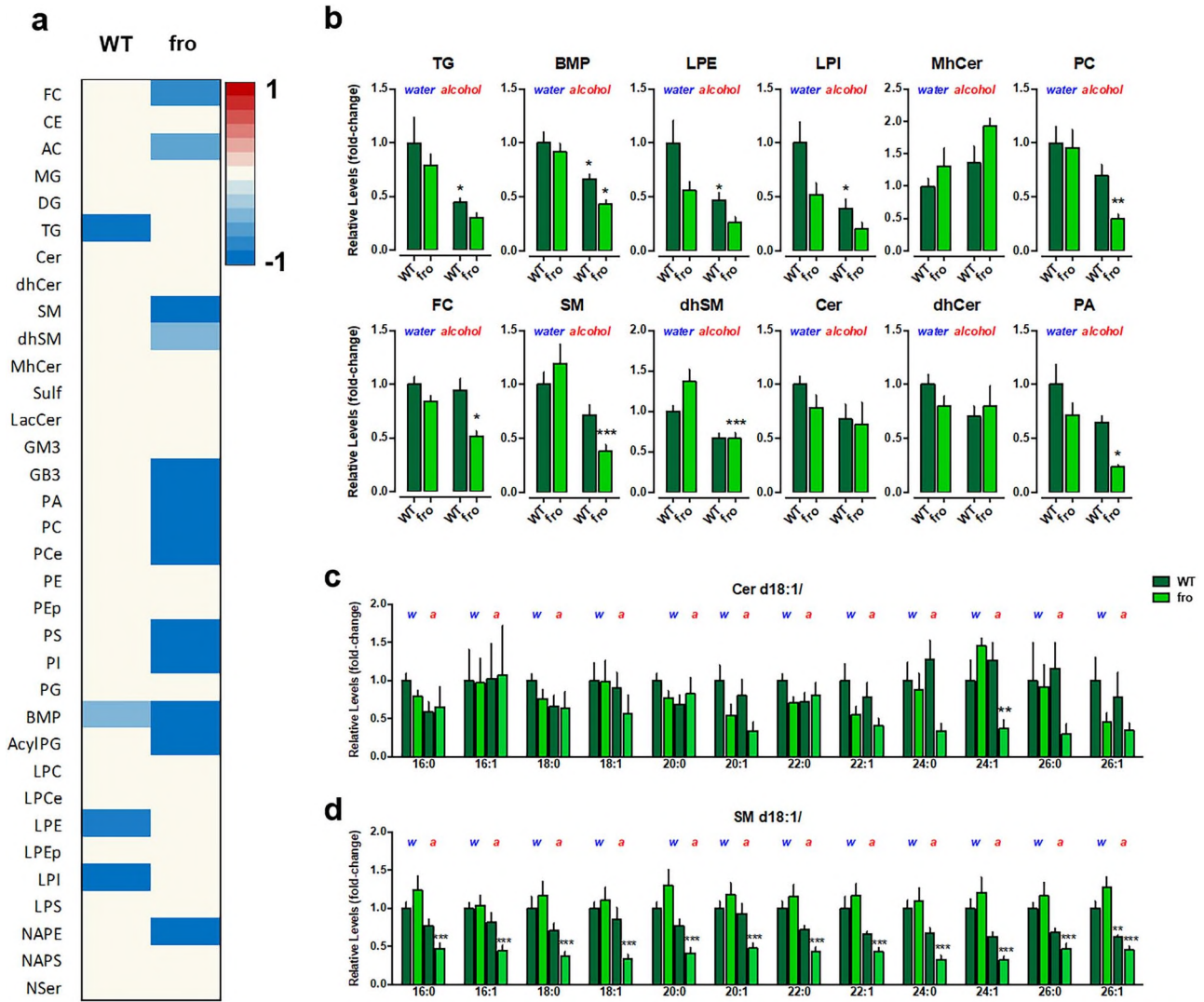


Fig. 5. Neutral sphingomyelinase determines alcohol effects on brain lipidome in males. (a) Lipidome heat map of chronic voluntary alcohol drinking effects in male mice with heterozygous NSM knock out (fro) and wild types (WT) controls (blue—significantly decreased levels, red—significantly increased levels; *t*-test vs. WT-water drinking). (b) Reduced NSM activity in male fro mice led only to an increase in total dhSM. Alcohol drinking caused significant decreases in total TG, dhSM, GB3, BMP, LPE, and LPI levels. This effect was amplified in male fro mice, which in addition showed also a decrease in FC, AC, DG, SM, LauCer, PA, PC, PCe, PS, PI, AcylPG, LPEp, and NAPE. There was also an increase in MhCer. (c) Target driven sphingolipid species analysis showed effects of fro and alcohol alone on single ceramide (Cer d18:1) species and an amplified sensitivity of fro mice for alcohol effects. (d) The fro mutation had no significant effects on sphingomyelin (SM) levels, but enhanced sensitivity to alcohol effects for all detected SM species (SM d18:1). All results show mean \pm SEM (* $P \leq 0.05$, ** $P \leq 0.01$, *** $P \leq 0.001$ vs. WT-water; FC, free cholesterol; CE, cholesterol ester; AC, acyl carnitine; MG, monoacylglycerol; DG, diacylglycerol; TG, triacylglycerol; Cer, ceramide; dhCer, dihydroceramide; SM, sphingomyelin; dhSM, dihydrosphingomyelin; MhCer, monohexosylceramide; Sulf, sulfate; LacCer, lactosylceramide; GM3, monosialodihexosylganglioside; GB3, Globotriaosylceramide; PA, phosphatidic acid; PC, Phosphatidylcholine; PCe, ether phosphatidylcholine, PE, phosphatidylethanolamine, PEp, plasmalogen phosphatidylethanolamine, PS, phosphatidylserine; PI, phosphatidylinositol; PG, phosphatidylglycerol; BMP, bis(monoacyl)glycerol; AcylPG, acyl Phosphatidylglycerol; LPC, lysophosphatidylcholine, LPCe, ether lysophosphatidylcholine; LPE, lysophosphatidylethanolamine; LPEp, plasmalogen lysophosphatidylethanolamine; LPI, lysophosphatidylinositol; LPS, Lysophosphatidylserine; NAPE, N-acyl phosphatidylethanolamine; NAPS, N-acyl phosphatidylserine; NSer, N-acyl serine).

in NSM null activity (Aubin et al. 2005; Stoffel et al. 2005). Here we asked whether the observed NSM role in sex-differences may also have a peripheral pathway involving bone–brain signaling. We used bone CT and measured whether attenuated NSM function would lead to any deficits in bone density. We found that the NSM activity deficit did not change bone density in male mice in the scalp, spinal cord, femur, tibia, humerus, and radius/ulna ($P > 0.05$; Fig. 6a–f). This is in line with previous reports on heterozygous fro mice, and in contrast to null mutations depleting the organism of all NSM activity and inducing

growth retardation and reduced bone mineralization (Aubin et al. 2005; Stoffel et al. 2005; Khavandgar et al. 2011). These findings confirm that a heterozygous NSM deletion is not sufficient to induce bone deficits in male mice.

Uncarboxylated osteocalcin is an inductor of bone mineralization in osteoblasts. Predominantly decarboxylated osteocalcin is released from osteoblast. Once released to the blood, osteocalcin reaches Gprc6a receptors in peripheral organs. It may also cross blood brain barrier and bind GPR158 and other receptors in

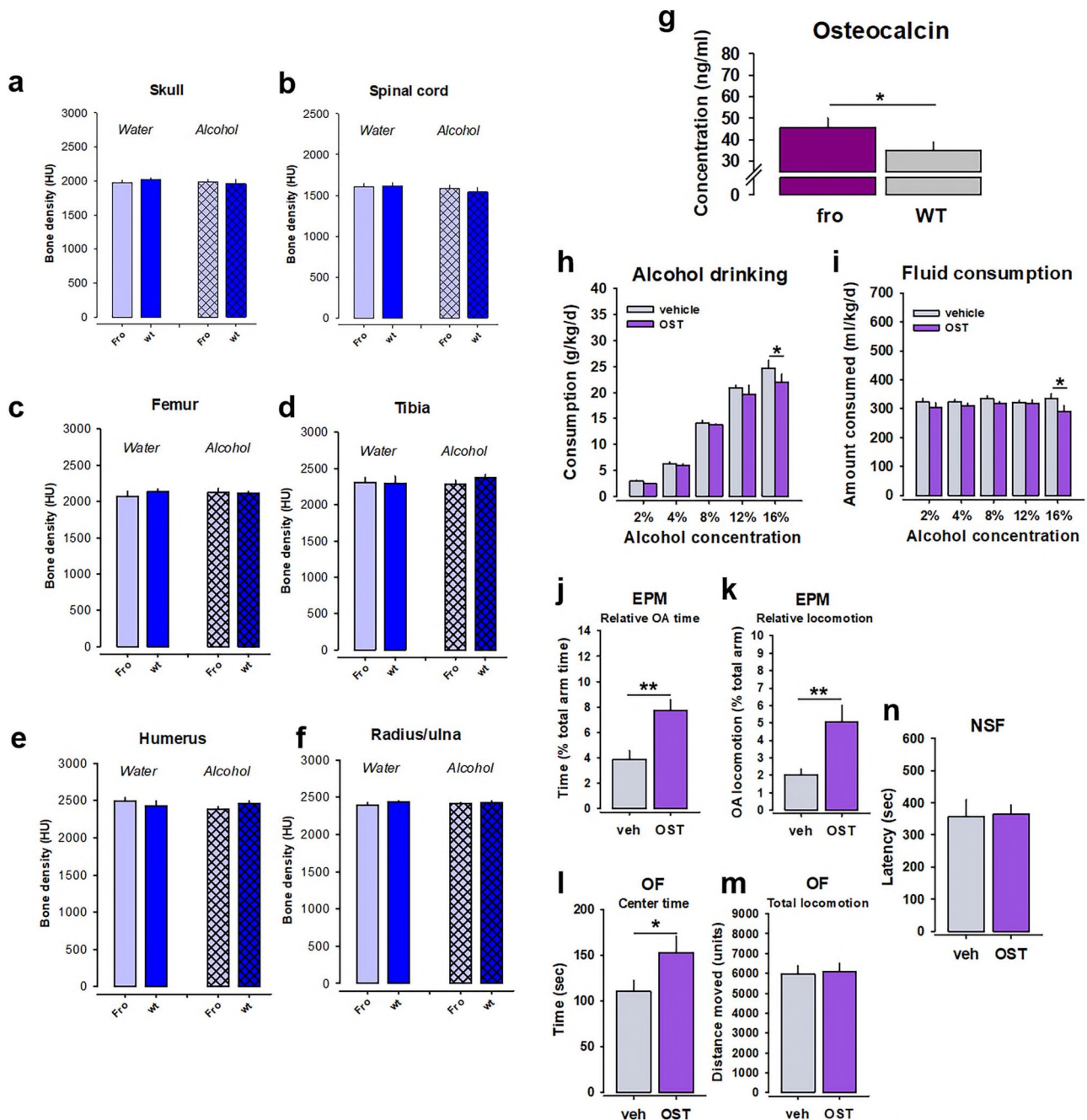


Fig. 6. Neutral sphingomyelinase control of alcohol consumption and emotional behavior by osteocalcin pathway. (a–f) Reduced function of neutral sphingomyelinase-2 (NSM) in male heterozygous NSM knock out (fro) mice has no effect on bone density, as measured with CT, compared to WT controls. Chronic voluntary alcohol consumption did not affect bone mineralization in male fro or WT mice. (g) Blood osteocalcin levels are upregulated in male fro mice compared to WT. (h) Chronic administration of osteocalcin (OSTEO; 0.03 $\mu\text{g}/30 \text{ g/h}$, i.p.) in male C57Bl6 mice for 28 days via osmotic mini-pumps attenuated alcohol consumption in a 2-bottle free-choice test, with (i) a small reduction in overall fluid intake. In male mice, OSTEO had an anxiolytic-like effect in (j, k) the EPM test and (l) the OF test without affecting (m) locomotor activity. (n) OSTEO had no effects on depression-related behavior in male mice in the NSF test. All results show mean \pm SEM (* $P \leq 0.05$, ** $P \leq 0.01$).

the brain. Peripheral osteocalcin action was linked to the acute stress response (Berger et al. 2019), while centrally acting osteocalcin can improve cognitive performance (Oury et al. 2013). Here we found that male fro mice show an upregulation of blood total osteocalcin levels ($t = 1.7970$, $P = 0.0457$; Fig. 6g). In order to test whether this signal would serve as an additional mediator of the NSM-induced alcohol drinking and emotional phenotype, we treated naïve C57Bl6J mice

for 28 days with bioactive mouse osteocalcin (0.03 $\mu\text{g}/\text{h}$, i.p.) using osmotic mini-pumps. In males, osteocalcin treatment reduced alcohol consumption (2-way ANOVA, factor treatment: $F_{1,13} = 2.351$, $P = 0.1491$, factor alcohol concentration: $F_{4,52} = 213.529$, $P < 0.0001$, interaction: $F_{4,52} = 0.719$, $P = 0.5825$; preplanned comparisons: 16%: $P = 0.0348$; Fig. 6h), but also total fluid consumption in a 2-bottle free-choice drinking test (2-way ANOVA, factor treatment: $F_{1,13} = 4.149$, $P = 0.0625$, factor alcohol

concentration: $F_{4,52} = 0.535$, $P = 0.7108$, interaction: $F_{4,52} = 0.972$, $P = 0.4306$; preplanned comparisons: 16%: $P = 0.0108$; Fig. 6i). Osteocalcin had anxiolytic-like effects in the EPM (relative arm time: $t = -3.6071$, $P = 0.0021$; relative arm locomotion: $t = -3.1390$, $P = 0.0047$; Fig. 6j and k) and OF ($t = -1.9480$, $P = 0.0366$; Fig. 6l), but no effect on depression-related behavior in the NSF test ($P > 0.05$; Fig. 6n; Supplementary Fig. 23). It did also not change locomotor activity ($P > 0.05$; Fig. 6m). As the osteocalcin effects dissociate from the fro behavioral phenotype, present findings may suggest that osteocalcin is a counter-regulatory signal that works to eliminate (bone) or restrict (behavior) the effects of NSM reduction.

Discussion

We discovered that spontaneous genetic variations in the *SMPD3* gene are related alcohol abuse and affective control in humans, which may further contribute to the shared genetic base of alcohol abuse and affective behavior (Mielenz et al. 2018; Walters et al. 2018; Zhou et al. 2020). *SMPD3* was selectively related to hippocampal size in the brain, but also to bone mineralization in the body periphery (Kalinichenko et al. 2021). Here we found in male mice that tonically reduced NSM activity enhanced alcohol consumption. Pharmacological NSM inhibition confirmed this role of NSM in alcohol drinking in males. In contrast, the NSM appeared to be required for the establishment, but not the expression of alcohol's conditioned rewarding effects. A delayed establishment of the conditioned reinforcing effects may be due to its role in spatial cue memory that depends in particular on NSM activity in the Nac and DH (Kalinichenko et al. 2020) and on AMPA and NMDA receptor formation (Wheeler et al. 2009; Tabatadze et al. 2010). However, the NSM is not required for the establishment of the conditioned reinforcing effects of a natural reinforcer.

The sphingolipids landscape has a profound effect on monoaminergic signaling in the brain, which can determine affective and cognitive behavior (Huston et al. 2016; Kalinichenko et al. 2020). Here we report a NSM control of dopaminergic and serotonergic signaling. In male mice, a reduced NSM activity attenuated 5-HT uptake and enhanced extracellular 5-HT activity in the Nac, while it attenuated spontaneous DA activity in the DH. This dissociating effect may result from distinct NSM regulation of DA and 5-HT uptake (Won et al. 2018). A previous study also showed reduction of DA uptake after reduced NSM inhibition in a PC12 cell model (Kim, Ahn, Ji, et al. 2010b). In the Nac, reduced NSM function potentiated the rather weak DA and 5-HT response to alcohol, which supports the reinforcing action and probably contributed to the enhanced alcohol drinking shown by these mice. A reduction of the 5-HT response to alcohol may be a reason for the delayed establishment of the spatial-related conditioned alcohol behaviors (Huston et al. 2013; Müller and Homberg 2015). Alcohol drinking enhanced 5-HT_{1A}-R and 5HT_{2C}-R, as well as DAT and SERT mRNA expression

in the DH. All those effects were absent in male mice with reduced NSM function. In that, reduced NSM function may provide a protection against chronic adaptations in the DA- and 5-HT-systems to alcohol exposure.

Reduced NSM activity led to a significantly enhanced level of depression- and anxiety-related behavior in male mice. Thereby, anxiety effects may be developmentally induced (Stoffel et al. 2005), as they did not occur after acute pharmacological NSM inhibition. Depressogenic effect, in contrast, have been also seen after acute NSM inhibition. Thus, there may also be an acute NSM influence on this behavior. This may be further supported by the effects of chronic stress, which eliminated the NSM-effects and caused a massive anxiety and depression-like response. The disadvantageous affective phenotype coincided with a reduced volume of the DH, vStr, and cerebellum. In particular, reduced capacity of the DH may render males more stress susceptible and facilitates depression-like behavior. In males, it was shown, that NSM is required for the excitability of hippocampal CA1 neurons (Norman et al. 2010). Chronically reduced NSM activity may, therefore, attenuated DH function at a large scale and drive depression- and anxiety like behavior.

Interestingly, male fro mice did not consume alcohol to self-manage their aversive emotional phenotype. Behavioral analysis showed that emotional behaviors were not affected after chronic alcohol drinking with self-titration. A previous study showed that a depressive/anxious phenotype induced by overexpression of ASM and resulting ceramide overload (Gulbins et al. 2013), may use alcohol to partially re-establish sphingolipid- and monoamine homeostasis in the Nac, and by that way, remit the aversive emotional phenotype (Müller et al. 2017; Müller and Kornhuber 2017). However, this mechanism was sex-dependent, predominantly emerging in females. While reduced NSM function induces a comparable phenotype in males, it has distinct effects on the lipidome and brain area development, for which further alcohol use may not be beneficial and rather work to worsen lipid allostasis. In male mice, voluntary alcohol drinking eliminated brain volume differences in the vStr and cerebellum. However, it further reduced DH volume in fro and WT mice. A reduction in NSM activity had little persistent effects on hippocampal neurogenesis in males. However, reduced NSM activity attenuated protective SOD activity against oxidative stress in the DH. This effect may contribute to an attenuated DH volume development in male fro mice.

The partial reduction of NSM activity caused a down regulation of TG, dhSM, GB3, BMP, LPE, and LPI in the Nac. The biggest effect, however, was seen in the susceptibility of the lipidome to chronic voluntary alcohol intake. This was much enhanced in males with reduced NSM activity. Now 19 of the 34 investigated lipid families were downregulated, and one upregulated. A single species analysis for Cer and SM species showed a significant decline of Cer 16:0 after alcohol consumption, which may support an antidepressant effect (Gulbins et al. 2013; Zoicas, Schumacher, et al. 2020). The decline of other

species, like Cer 20:1, Cer 22:1, and Cer 24:0, may suggest enhanced plasticity and learning in male mice (Huston et al. 2016). It should be noted that this was the effects of chronic voluntary alcohol consumption with permanent alcohol access and the possibility of self-titration. Binge consumption of alcohol over short periods of time, however, was shown to yield a rather different pattern of Cer responses in the cortex of male rats. This is dominated by an acute decline in several desaturated Cer species and MhCer species, and an increase in Cer during withdrawal (Bae et al. 2014; Roux et al. 2015). A generally favorable effect of alcohol drinking on forebrain total Cer levels was previously suggested by Godfrey et al. (2015), that was possibly mediated by a downregulation of sphingolipid delta(4)-desaturase. As such, alcohol appears to have a unique effect on the brain sphingolipidome, which may directly affect drinking behavior, but to a smaller extent emotional behavior, in males.

Male mice with reduced NSM function did not show deficits in bone integrity, but an upregulation of blood osteocalcin levels. Chronic osteocalcin treatment in naïve mice, however, did not mimic the male mice phenotype of enhanced alcohol consumption, but rather showed similar effects as in females (Kalinichenko et al. 2021). This may suggest that the peripheral osteocalcin response counteracts central effects of NSM on alcohol consumption in males. This effect is in line with findings from male osteocalcin knock out mice, which showed an enhanced alcohol consumption (Patterson-Buckendahl et al. 2018). Also the effects of osteocalcin on affective behavior were different from females. In males, osteocalcin had a clear anxiolytic effect, but no effect on depression-like behavior. As such, peripheral osteocalcin may also counteract central NSM effects on affective behavior in males. Altogether, the findings suggest that SMPD3 and NSM control alcohol drinking and the emotional behavior in males by several central mechanisms, which are partly attenuated by peripheral, bone-mediated action.

An important finding of this study is that although SMPD3 and NSM are associated with alcohol abuse behaviors, depression/anxiety as well as bone mineralization. The neurobiological mechanisms of this association differ remarkably between males and females. Female mice with attenuated NSM function showed reduced anxiety and depression, as well as a reduced alcohol consumption. This protection may be mediated by enhanced volume of DH and insular cortex in female mice. This advantage, however disappeared after chronic alcohol consumption together with behavioral protection and benefits. In females, lack of NSM function did not affect lipidomic regulation very much (Kalinichenko et al. 2021). As such, centrally acting mechanisms of NSM controlling emotional and addiction-like behavior show a considerable sex-dimorphism. Not so peripheral effects of the NSM, when they provoked counter regulatory processes affecting

behavioral control by an indirect pathway. An NSM reduction led to a compensatory osteocalcin response, which is most likely responsible for maintenance of bone integrity in the partial absence of NSM a key factor for bone mineralization (Aubin et al. 2005). Once released into the blood it can reach the brain and bind to osteocalcin- and orphan-receptors (Obri et al. 2018). Behavioral effects of this bone-brain communication were shown for learning and memory as well as in emotional behavior, but in females only (Oury et al. 2013; Khrimian et al. 2017). We found that this osteocalcin response has similar effects in males and females, in that it attenuates alcohol consumption and reduces anxiety-(males) and depression (females)-related behaviors. Anxiolytic effects of osteocalcin were reported in female mice in a previous study, which were mediated by brain GPR158 receptors (Khrimian et al. 2017).

The observed gender-specific differences of NSM involvement in the control of affective behavior might be related to the interaction between the ceramide system and sex hormones. Clinical studies showed that blood levels of ceramides, particularly long-chain ceramides, differ in a gender-specific way (Ishikawa et al. 2013; Weir et al. 2013; Mielke et al. 2015), and might correlate with circulating levels of estradiol in women (Pan et al. 2014; Yu et al. 2015). In vitro studies showed that estradiol downregulated ceramide levels probably via the suppression of de novo ceramide synthesis pathway (Pan et al. 2014; Yu et al. 2015; Vozella et al. 2019). The gender-specific differences in ceramide levels might be followed by changes in the receptor functioning, which may in turn affect the behavioral patterns. Particularly, the study of Kalinichenko et al. (2020) revealed profound sex-differences in the NSM contribution to various types of memory based on the differences in NMDA receptor functioning.

In summary, we demonstrate a role for the NSM in alcohol consumption and conditioned alcohol effects, as well as in affective behavior in males. Thereby, no alcohol use for self-medication of an aversive affective state was observed under NSM control. The observed effects on alcohol consumption may be mediated by an NSM control of acute and chronic monoaminergic responses and lipidomic adaptations to alcohol exposure. Counter-regulatory action emerged, driven by peripheral NSM effects on bone-brain signaling with osteocalcin. Importantly, central, but not peripheral NSM action appeared to be highly sex-dependent and may serve as a key mechanism for the sex differences in alcohol abuse and instrumentalization. Our data support the idea of targeting NSM activity in a sex-specific treatment approach of alcohol abuse that involves affective disorder symptoms.

Authors' contributions

L.S.K. and C.P.M. initiated the study, designed experiments, supervised research, and wrote the manuscript. C.M., B.L., J.K., N.T., T.J., G.S., L.S.K., F.A., M.D., A.L.E., J.G.,

L.A.H., M.H., J.H., S.E.H., G.K., L.L., C.L., D.M., N.K.S., M.P., F.U., F.V., E.W., M.W., A.L., P.K., A.E., V.E., D.N.M., M.D.L., J.P.H., and C.P.M. performed behavioral and functional studies. C.R. performed gene expression studies. C. McV. and J.H. performed uptake measurements. I.S., M.F., and M.F. performed oxidative stress studies. S.K., L.S.K., L.M., R. F, S.M.T., N.P.S., and A.F. performed the neurogenesis study. E.M.S. and C.A. provided a test compound. L.S.K. and A.B. performed osteocalcin measurements. C.S., J.S., L.S.K., I.W., S.K., T.B., and A.H. performed MRI experiments. A.M. and T.O. performed lipidomic analysis. All authors discussed the results and commented on the manuscript.

Acknowledgments

The authors like to thank Laura Emrich, Jana Schramm, Sandra Strobel, Franziska Kress, Hedy Riesop, and Marcel-René Muschler for excellent technical assistance.

Supplementary material

Supplementary material is available at *Cerebral Cortex Journal* online.

Funding

This work was supported by the German National Science Foundation (Deutsche Forschungsgemeinschaft [DFG]), grant MU 2789/8-2, KO 947/13-3, KO 947/15-2, HU 306/27-3, and TRR265 (Project-ID 402170461), the Johannes und Frieda Marohn-Stiftung, the statutory funds of the Maj Institute of Pharmacology Polish Academy of Sciences, and by bilateral cooperation (no. PPN/BIL/2018/1/00004) between the Polish National Agency for Academic Exchange (NAWA) and the German Academic Exchange Service (DAAD), and in part by the Federal Ministry of Education and Research (BMBF) under the e: Med Program (031L0190B and 01KC2004B). C. Mühle, A. F, and J.K. are PIs and L.M., N.P.S. are fellows of the research training group 2162 funded by the DFG grant 270949263/GRK2162/1 and GRK2162/2. This project was in partial fulfillment of the requirements for obtaining the degree “Dr med.” by F.A., M.D., A.L.E., J.G., M.H., J.H., S.K., L.L., C.L., D.M., N.K.S., C.S., J.S., F.U., F.V., E.W., M.W., S.M.T., and PhD by N.T.

Conflict of interest statement. The authors declare no competing financial interests.

References

- Airola MV, Hannun YA. Sphingolipid metabolism and neutral sphingomyelinases. *Handb Exp Pharmacol.* 2013;215:57–76.
- Airola MV, Shanbhogue P, Shamseddine AA, Guja KE, Senkal CE, Maini R, Bartke N, Wu BX, Obeid LM, Garcia-Diaz M, et al. Structure of human nSMase2 reveals an interdomain allosteric activation mechanism for ceramide generation. *Proc Natl Acad Sci U S A.* 2017;114:E5549–E5558.
- Amato D, Canneva F, Cumming P, Maschauer S, Groos D, Dahlmanns JK, Grömer TW, Chiofalo L, Dahlmanns M, Zheng F, et al. A dopaminergic mechanism of antipsychotic drug efficacy, failure, and failure reversal: the role of the dopamine transporter. *Mol Psychiatry.* 2020;25:2101–2018.
- Aubin I, Adams CP, Opsahl S, Septier D, Bishop CE, Auge N, Salvayre R, Negre-Salvayre A, Goldberg M, Guénet JL, et al. A deletion in the gene encoding sphingomyelin phosphodiesterase 3 (Smpd3) results in osteogenesis and dentinogenesis imperfecta in the mouse. *Nat Genet.* 2005;37(8):803–805.
- Bae M, Bandaru VV, Patel N, Haughey NJ. Ceramide metabolism analysis in a model of binge drinking reveals both neuroprotective and toxic effects of ethanol. *J Neurochem.* 2014;131:645–654.
- Berger JM, Singh P, Khirmian L, Morgan DA, Chowdhury S, Arteaga-Solis E, Horvath TL, Domingos AI, Marsland AL, Yadav VK, et al. Mediation of the acute stress response by the skeleton. *Cell Metab.* 2019;30:890–902.
- Bjork K, Sjogren B, Svenningsson P. Regulation of serotonin receptor function in the nervous system by lipid rafts and adaptor proteins. *Exp Cell Res.* 2010;316:1351–1356.
- Bligh EG, Dyer WJ. A rapid method of total lipid extraction and purification. *Can J Biochem Physiol.* 1959;37(8):911–917.
- Brown E, Mc Veigh CJ, Santos L, Gogarty M, Müller HK, Elfving B, Brayden DJ, Haase J. TNF α -dependent anhedonia and upregulation of hippocampal serotonin transporter activity in a mouse model of collagen-induced arthritis. *Neuropharmacology.* 2018;137:211–220.
- Carroll ME, Lynch WJ. How to study sex differences in addiction using animal models. *Addict Biol.* 2016;21:1007–1029.
- Chan RB, Oliveira TG, Cortes EP, Honig LS, Duff KE, Small SA, Wenk MR, Shui G, Di Paolo G. Comparative lipidomic analysis of mouse and human brain with Alzheimer disease. *J Biol Chem.* 2012;287(4):2678–2688.
- Easton AC, Lucchesi W, Lourdasamy A, Lenz B, Solati J, Golub Y, Lewczuk P, Fernandes C, Desrivieres S, Dawirs RR, et al. α CaMKII autophosphorylation controls the establishment of alcohol drinking behavior. *Neuropsychopharmacology.* 2013;38(9):1636–1647.
- Easton AC, Lucchesi W, Mizuno K, Fernandes C, Schumann G, Giese KP, Müller CP. α CaMKII autophosphorylation controls the establishment of alcohol-induced conditioned place preference in mice. *Behav Brain Res.* 2013;252:72–76.
- Fantini J, Barrantes FJ. Sphingolipid/cholesterol regulation of neurotransmitter receptor conformation and function. *Biochim Biophys Acta.* 2009;1788:2345–2361.
- Filosto S, Fry W, Knowlton AA, Goldkorn T. Neutral sphingomyelinase 2 (nSMase2) is a phosphoprotein regulated by calcineurin (PP2B). *J Biol Chem.* 2010;285:10213–10222.
- Franklin KBJ, Paxinos G. *The mouse brain in stereotaxic coordinates.* San Diego: Academic Press; 1997
- GBD. The global burden of disease attributable to alcohol and drug use in 195 countries and territories, 1990–2016: a systematic analysis for the global burden of disease study 2016. *Lancet Psychiatry.* 2018;5:987–1012.
- Godfrey J, Jeanguenin L, Castro N, Olney JJ, Dudley J, Pipkin J, Walls SM, Wang W, Herr DR, Harris GL, et al. Chronic voluntary ethanol consumption induces favorable ceramide profiles in selectively bred alcohol-preferring (P) rats. *PLoS One.* 2015;10:e0139012.
- Guan Z, Li S, Smith DC, Shaw WA, Raetz CR. Identification of N-acylphosphatidylserine molecules in eukaryotic cells. *Biochemistry.* 2007;46(50):14500–14513.
- Gulbins E, Palmada M, Reichel M, Lüth A, Böhmer C, Amato D, Müller CP, Tischbirek CH, Groemer TW, Tabatabai G, et al. Acid

- sphingomyelinase-ceramide system mediates effects of antidepressant drugs. *Nat Med*. 2013;19:934–938.
- Gulbins A, Schumacher F, Becker KA, Wilker B, Soddemann M, Boldrin F, Müller CP, Edwards MJ, Goodman M, Caldwell CC, et al. Antidepressants act by inducing autophagy controlled by sphingomyelin-ceramide. *Mol Psychiatry*. 2018;23:2324–2346.
- Hannun YA, Obeid LM. Principles of bioactive lipid signalling: lessons from sphingolipids. *Nat Rev Mol Cell Biol*. 2008;9:139–150.
- He J, Nixon K, Shetty AK, Crews FT. Chronic alcohol exposure reduces hippocampal neurogenesis and dendritic growth of newborn neurons. *Eur J Neurosci*. 2005;21:2711–2720.
- Hess A, Kress S, Rakete S, Muench G, Kornhuber J, Pischetsrieder M, Müller CP. Influence of the fat/carbohydrate component of snack food on energy intake pattern and reinforcing properties in rodents. *Behav Brain Res*. 2019;364:328–333.
- Hilderbrand ER, Lasek AW. Studying sex differences in animal models of addiction: an emphasis on alcohol-related behaviors. *ACS Chem Neurosci*. 2018;9:1907–1916.
- Holthuis JC, Pomorski T, Raggars RJ, Sprong H, Van Meer G. The organizing potential of sphingolipids in intracellular membrane transport. *Physiol Rev*. 2001;81:1689–1723.
- Hsu FF, Turk J, Shi Y, Groisman EA. Characterization of acylphosphatidylglycerols from salmonella typhimurium by tandem mass spectrometry with electrospray ionization. *J Am Soc Mass Spectrom*. 2004;15(1):1–11.
- Huston JP, de Souza Silva MA, Topic B, Müller CP. What's conditioned in conditioned place preference? *Trends Pharmacol Sci*. 2013;34(3):162–166.
- Huston JP, Kornhuber J, Mühle C, Japtok L, Komorowski M, Mattern C, Reichel M, Gulbins E, Kleuser B, Topic B, et al. A sphingolipid mechanism for behavioral extinction. *J Neurochem*. 2016;137:589–603.
- Ishikawa M, Tajima Y, Murayama M, Senoo Y, Maekawa K, Saito Y. Plasma and serum from nonfasting men and women differ in their lipidomic profiles. *Biol Pharm Bull*. 2013;36:682–685.
- Kalinichenko LS, Hammad L, Reichel M, Kohl Z, Gulbins E, Kornhuber J, Müller CP. Acid sphingomyelinase controls dopamine activity and responses to appetitive stimuli in mice. *Brain Res Bull*. 2019;146:310–319.
- Kalinichenko LS, Abdel-Hafiz L, Wang AL, Mühle C, Rösel N, Schumacher F, Kleuser B, Smaga I, Frankowska M, Filip M, et al. Neutral sphingomyelinase is an affective valence-dependent regulator of learning and memory. *Cereb Cortex*. 2020;31(2):1316–1333.
- Kalinichenko LS, Mühle C, Jia T, Anderheiden F, Datz M, Eberle AL, Eulenburg V, Granzow J, Hofer M, Hohenschild J, et al. Neutral sphingomyelinase mediates the co-morbidity trias of alcohol abuse, major depression and bone defects. *Mol Psychiatry*. 2021;26(12):7403–7416.
- Khavandgar Z, Poirier C, Clarke CJ, Li J, Wang N, McKee MD, Hannun YA, Murshed M. A cell-autonomous requirement for neutral sphingomyelinase 2 in bone mineralization. *J Cell Biol*. 2011;194:277–289.
- Khrimian L, Obri A, Ramos-Brossier M, Rousseaud A, Moriceau S, Nicot AS, Mera P, Kosmidis S, Karnavas T, Saudou F, et al. Gpr158 mediates osteocalcin's regulation of cognition. *J Exp Med*. 2017;214:2859–2873.
- Kim SK, Ahn KH, Jeon HJ, Lee DH, Jung SY, Jung KM, Kim DK. Purification of neutral sphingomyelinase 2 from bovine brain and its calcium-dependent activation. *J Neurochem*. 2010a;112:1088–1097.
- Kim SK, Ahn KH, Ji JE, Choi JM, Jeon HJ, Jung SY, Jung KM, Kim DK. Neutral sphingomyelinase 2 induces dopamine uptake through regulation of intracellular calcium. *Cell Signal*. 2010b;22:865–870.
- Kornhuber J, Müller CP, Becker KA, Reichel M, Gulbins E. The ceramide system as a novel antidepressant target. *Trends Pharmacol Sci*. 2014;35:293–304.
- Krishnan V, Nestler EJ. The molecular neurobiology of depression. *Nature*. 2008;455:894–902.
- Le Maitre TW, Dhanabalan G, Bogdanovic N, Alkass K, Druid H. Effects of alcohol abuse on proliferating cells, stem/progenitor cells, and immature neurons in the adult human hippocampus. *Neuropsychopharmacology*. 2018;43:690–699.
- Magnani F, Tate CG, Wynne S, Williams C, Haase J. Partitioning of the serotonin transporter into lipid microdomains modulates transport of serotonin. *J Biol Chem*. 2004;279:38770–38778.
- van Meer G, Voelker DR, Feigenson GW. Membrane lipids: where they are and how they behave. *Nat Rev Mol Cell Biol*. 2008;9:112–124.
- Mielenz D, Reichel M, Jia T, Quinlan EB, Stöckl T, Mettang M, Zilske D, Kirmizi-Alsan E, Schönberger P, Praetner M, et al. EFhd2/Swiprosin-1 is a common genetic determinant for sensation seeking/low anxiety and alcohol addiction. *Mol Psychiatry*. 2018;23(5):1303–1319.
- Mielke MM, Bandaru VVR, Han D, An Y, Resnick SM, Ferrucci L, Haughey NJ. Demographic and clinical variables affecting mid-to late-life trajectories of plasma ceramide and dihydroceramide species. *Aging Cell*. 2015;14:1014–1023.
- Mühle C, Kornhuber J. Assay to measure sphingomyelinase and ceramidase activities efficiently and safely. *J Chromat A*. 2017;1481:137–144.
- Müller CP. Drug instrumentalization. *Behav Brain Res*. 2020;390:112672.
- Müller CP, Homberg JR. The role of serotonin in drug use and addiction. *Behav Brain Res*. 2015;277:146–192.
- Müller CP, Kornhuber J. Biological evidence for paradoxical improvement of psychiatric disorder symptoms by addictive drugs. *Trends Pharmacol Sci*. 2017;38:501–502.
- Müller CP, Schumann G. Drugs as instruments: a new framework for non-addictive psychoactive drug use. *Behav Brain Sci*. 2011a;34:293–310.
- Müller CP, Schumann G. To use or not to use: expanding the view on non-addictive psychoactive drug consumption and its implications. *Behav Brain Sci*. 2011b;34:328–347.
- Müller CP, Kalinichenko LS, Tiesel J, Witt M, Stöckl T, Sprenger E, Fuchser J, Beckmann J, Praetner M, Huber SE, et al. Paradoxical antidepressant effects of alcohol are related to acid sphingomyelinase and its control of sphingolipid homeostasis. *Acta Neuropathol*. 2017;133(3):463–483.
- Müller CP, Chu C, Qin L, Liu C, Xu B, Gao H, Ruggeri B, Hieber S, Schneider J, Jia T, et al. The cortical neuroimmune regulator TANK affects emotional processing and enhances alcohol drinking: a translational study. *Cereb Cortex*. 2019;29:1736–1751.
- Müller CP, Mühle C, Kornhuber J, Lenz B. Sex-dependent alcohol instrumentalization goals in non-addicted alcohol consumers versus patients with alcohol use disorder: longitudinal change and outcome prediction. *Alcohol Clin Exp Res*. 2021;45(3):577–586.
- Nixon K, Crews FT. Binge ethanol exposure decreases neurogenesis in adult rat hippocampus. *J Neurochem*. 2002;83:1087–1093.
- Norman E, Cutler RG, Flannery R, Wang Y, Mattson MP. Plasma membrane sphingomyelin hydrolysis increases hippocampal neuron excitability by sphingosine-1-phosphate mediated mechanisms. *J Neurochem*. 2010;114:430–439.

- Obri A, Khirmian L, Karsenty G, Oury F. Osteocalcin in the brain: from embryonic development to age-related decline in cognition. *Nat Rev Endocrinol*. 2018;14:174–182.
- Oliveira TG, Chan RB, Bravo FV, Miranda A, Silva RR, Zhou B, Marques F, Pinto V, Cerqueira JJ, Di Paolo G, et al. The impact of chronic stress on the rat brain lipidome. *Mol Psychiatry*. 2016;21:80–88.
- Oury F, Khirmian L, Denny CA, Gardin A, Chamouni A, Goeden N, Huang YY, Lee H, Srinivas P, Gao XB, et al. Maternal and offspring pools of osteocalcin influence brain development and functions. *Cell*. 2013;155:228–241.
- Pan W, Yu J, Shi R, Yan L, Yang T, Li Y, Zhang Z, Yu G, Bai Y, Schuchman EH, et al. Elevation of ceramide and activation of secretory acid sphingomyelinase in patients with acute coronary syndromes. *Coron Artery Dis*. 2014;25:230–235.
- Patterson-Buckendahl P, Shahid M, Shah A, Pohorecky LA. Altered ethanol consumption in Osteocalcin null mutant mice. *Cell Mol Neurobiol*. 2018;38(1):261–271.
- Pum M, Huston JP, Müller CP. The role of cortical serotonin in anxiety. *Behav Neurosci*. 2009;123(2):449–454.
- Ramsey PH. Multiple comparisons of independent means. In: Edwards LK, editors. *Applied analysis of variance in behavioral science*. New York: Marcel Dekker; 1993. pp. 25–61
- Roux A, Muller L, Jackson SN, Baldwin K, Womack V, Pagiazitis JG, O'Rourke JR, Thanos PK, Balaban C, Schultz JA, et al. Chronic ethanol consumption profoundly alters regional brain ceramide and sphingomyelin content in rodents. *ACS Chem Neurosci*. 2015;6:247–259.
- Sanchis-Segura C, Becker JB. Why we should consider sex (and study sex differences) in addiction research. *Addict Biol*. 2016;21:995–1006.
- Schneider M, Levant B, Reichel M, Gulbins E, Kornhuber J, Müller CP. Lipids in psychiatric disorders and preventive medicine. *Neurosci Biobehav Rev*. 2017;76:336–362.
- Smaga I, Pomierny B, Krzyżanowska W, Pomierny-Chamioło L, Miszkiel J, Niedzielska E, Ogórka A, Filip M. N-acetylcysteine possesses antidepressant-like activity through reduction of oxidative stress: behavioral and biochemical analyses in rats. *Prog Neuro-Psychopharmacol Biol Psychiatry*. 2012;39:280–287.
- Spanagel R. Alcoholism: a systems approach from molecular physiology to addictive behavior. *Physiol Rev*. 2009;89:649–705.
- Stoffel W, Jenke B, Block B, Zumbansen M, Koebke J. Neutral sphingomyelinase 2 (smpd3) in the control of postnatal growth and development. *Proc Natl Acad Sci U S A*. 2005;102:4554–4559.
- Stranahan AM, Cutler RG, Button C, Telljohann R, Mattson MP. Diet-induced elevations in serum cholesterol are associated with alterations in hippocampal lipid metabolism and increased oxidative stress. *J Neurochem*. 2011;118:611–615.
- Tabatadze N, Savonenko A, Song H, Bandaru VV, Chu M, Haughey NJ. Inhibition of neutral sphingomyelinase-2 perturbs brain sphingolipid balance and spatial memory in mice. *J Neurosci Res*. 2010;88:2940–2951.
- Turner S, Mota N, Bolton J, Sareen J. Self-medication with alcohol or drugs for mood and anxiety disorders: a narrative review of the epidemiological literature. *Depress Anxiety*. 2018;35:851–860.
- Vozella V, Basit A, Piras F, Realini N, Armirotti A, Bossù P, Assogna F, Sensi SL, Spalletta G, Piomelli D. Elevated plasma ceramide levels in post-menopausal women: a cross-sectional study. *Aging (Albany NY)*. 2019;11:73–88.
- Walker DW, Barnes DE, Zornetzer SF, Hunter BE, Kubanis P. Neuronal loss in hippocampus induced by prolonged ethanol consumption in rats. *Science*. 1980;209:711–713.
- Walters RK, Polimanti R, Johnson EC, McClintick JN, Adams MJ, Adkins AE, Aliev F, Bacanu SA, Batzler A, Bertelsen S, et al. Transancestral GWAS of alcohol dependence reveals common genetic underpinnings with psychiatric disorders. *Nat Neurosci*. 2018;21:1656–1669.
- Wang AL, Chao OY, Yang YM, Trossbach SV, Müller CP, Korth C, Huston JP, de Souza Silva MA. Anxiogenic-like behavior and deficient attention/working memory in rats expressing the human DISC1 gene. *Pharmacol Biochem Behav*. 2019;179:73–79.
- Weir JM, Wong G, Barlow CK, Greeve MA, Kowalczyk A, Almasy L, Comuzzie AG, Mahaney MC, Jowett JBM, Shaw J, et al. Plasma lipid profiling in a large population-based cohort. *J Lipid Res*. 2013;54:2898–2908.
- Wheeler D, Knapp E, Bandaru VV, Wang Y, Knorr D, Poirier C, Mattson MP, Geiger JD, Haughey NJ. Tumor necrosis factor- α -induced neutral sphingomyelinase-2 modulates synaptic plasticity by controlling the membrane insertion of NMDA receptors. *J Neurochem*. 2009;109:1237–1249.
- Won JH, Kim SK, Shin IC, Ha HC, Jang JM, Back MJ, Kim DK. Dopamine transporter trafficking is regulated by neutral sphingomyelinase 2/ceramide kinase. *Cell Signal*. 2018;44:171–187.
- Yu J, Pan W, Shi R, Yang T, Li Y, Yu G, Bai Y, Schuchman EH, He X, Zhang G. Ceramide is upregulated and associated with mortality in patients with chronic heart failure. *Can J Cardiol*. 2015;31:357–363.
- Zhang J, Jiao J. Molecular biomarkers for embryonic and adult neural stem cell and neurogenesis. *Biomed Res Int*. 2015:727542.
- Zheng F, Puppel A, Huber SE, Link AS, Eulenburg V, van Brederode JF, Müller CP, Alzheimer C. Activin controls ethanol potentiation of inhibitory synaptic transmission through GABAA receptors and concomitant behavioral sedation. *Neuropsychopharmacology*. 2016;41(8):2024–2033.
- Zhou H, Sealock JM, Sanchez-Roige S, Clarke TK, Levey DF, Cheng Z, Li B, Polimanti R, Kember RL, Smith RV, et al. Genome-wide meta-analysis of problematic alcohol use in 435,563 individuals yields insights into biology and relationships with other traits. *Nat Neurosci*. 2020;23:809–818.
- Zoicas I, Huber SE, Kalinichenko LS, Gulbins E, Müller CP, Kornhuber J. Ceramides affect alcohol consumption and depressive-like and anxiety-like behavior in a brain region- and ceramide species-specific way in male mice. *Addict Biol*. 2020;25(6):e12847.
- Zoicas I, Schumacher F, Kleuser B, Reichel M, Gulbins E, Fejtova A, Kornhuber J, Rhein C. The forebrain-specific overexpression of acid sphingomyelinase induces depressive-like symptoms in mice. *Cell*. 2020;9(5):1244.